Artificial intelligence for diagnosing acute stroke: a 25-year retrospective

Zhaoxin Wang, Wenwen Yang, Zhengyu Li, Ze Rong, Xing Wang, Jincong Han, Lei Ma

Submitted to: Journal of Medical Internet Research
on: April 20, 2024

Table of Contents

Artificial intelligence for diagnosing acute stroke: a 25-year retrospective

Zhaoxin Wang[1]; Wenwen Yang[1]; Zhengyu Li[1]; Ze Rong[1]; Xing Wang[1]; Jincong Han[1]; Lei Ma[2]

[1]Nantong University Nantong CN

Corresponding Author:
Lei Ma

Abstract

Background: Stroke is a leading cause of death and disability in the world. Rapid and accurate diagnosis is crucial for minimizing brain damage and optimize treatment plans.

Objective: This review aims to summarize the methods of artificial intelligence (AI) assisted diagnosis of acute stroke and the assessment of stroke prognosis over the past 25 years, providing an overview of common performance metrics and the development trends of algorithms. It also delves into existing issues and future prospects, intending to provide a comprehensive reference for clinical practice.

Methods: Method: A total of 33 representative articles published between 1999 and 2024 on utilizing AI technology for acute stroke diagnosis were systematically selected and analyzed in detail. Results: Results: The segmentation of acute stroke lesions from 1999 to 2024 can be divided into three stages. Prior to 2012, research mainly focused on brain white matter segmentation using thresholding techniques. From 2012 to 2016, the focus shifted to stroke lesion segmentation based on machine learning (ML). After 2016, the emphasis was on deep learning (DL) based stroke lesion segmentation, with a significant improvement in accuracy observed. For the classification and prognosis assessment of strokes, both ML and DL have their advantages, achieving a high level of accuracy. Conclusions: Conclusion: Over the past 25 years, AI technology has shown promising performance in segmenting, classifying, and assessing the prognosis of acute stroke lesion.

Method: A total of 33 representative articles published between 1999 and 2024 on utilizing AI technology for acute stroke diagnosis were systematically selected and analyzed in detail.

Results: The segmentation of acute stroke lesions from 1999 to 2024 can be divided into three stages. Prior to 2012, research mainly focused on brain white matter segmentation using thresholding techniques. From 2012 to 2016, the focus shifted to stroke lesion segmentation based on machine learning (ML). After 2016, the emphasis was on deep learning (DL) based stroke lesion segmentation, with a significant improvement in accuracy observed. For the classification and prognosis assessment of strokes, both ML and DL have their advantages, achieving a high level of accuracy.

Conclusions: Conclusion: Over the past 25 years, AI technology has shown promising performance in segmenting, classifying, and assessing the prognosis of acute stroke lesion.

Conclusion: Over the past 25 years, AI technology has shown promising performance in segmenting, classifying, and assessing the prognosis of acute stroke lesion.

(JMIR Preprints 20/04/2024:59711)
DOI: https://doi.org/10.2196/preprints.59711

Preprint Settings

1) Would you like to publish your submitted manuscript as preprint?

✓ **Please make my preprint PDF available to anyone at any time (recommended).**
Please make my preprint PDF available only to logged-in users; I understand that my title and abstract will remain visible to all users.
Only make the preprint title and abstract visible.
No, I do not wish to publish my submitted manuscript as a preprint.

2) If accepted for publication in a JMIR journal, would you like the PDF to be visible to the public?

✓ **Yes, please make my accepted manuscript PDF available to anyone at any time (Recommended).**
Yes, but please make my accepted manuscript PDF available only to logged-in users; I understand that the title and abstract will remain v

Yes, but only make the title and abstract visible (see Important note, above). I understand that if I later pay to participate in <a href="http

Original Manuscript

Artificial intelligence for diagnosing acute stroke: a 25-year retrospective

School of Information Science and Technology, Nantong University, Nantong 226019, Jiangsu Province, China

Abstract

Background: Stroke is a leading cause of death and disability worldwide. Rapid and accurate diagnosis is crucial for minimizing brain damage and optimizing treatment plans. **Objective**: This review aims to summarize the methods of artificial intelligence (AI)-assisted stroke diagnosis over the past 25 years, providing an overview of performance metrics and algorithm development trends. It also delves into existing issues and future prospects, intending to offer a comprehensive reference for clinical practice. **Method**: A total of 50 representative articles published between 1999 and 2024 on utilizing AI technology for stroke prevention and diagnosis were systematically selected and analyzed in detail. **Results**: AI-assisted stroke diagnosis has made significant advancements in stroke lesion segmentation and classification, stroke risk prediction, and stroke prognosis. Prior to 2012, research mainly focused on segmentation using traditional thresholding and heuristic techniques. From 2012 to 2016, the focus shifted to machine learning (ML)-based approaches. After 2016, the emphasis moved to deep learning (DL), which brought significant improvements in accuracy. In stroke lesion segmentation and classification, and stroke risk prediction, DL has shown superiority over ML. In stroke prognosis, both DL and ML have shown good performance. **Conclusion**: Over the past 25 years, AI technology has shown promising performance in stroke diagnosis.

Keywords: Acute stroke; Artificial intelligence; Machine learning; Deep learning; Stroke lesion segmentation and classification; Stroke prediction; Stroke prognosis.

1 Introduction

Stroke is a global public health issue, ranking as the second leading cause of death and the third leading cause of disability and death. One in every four people over the age of 25 will experience a stroke in their lifetime. 11.6% of deaths are due to stroke, and both the incidence, mortality and disability rates of stroke are on the rise [1–3].

Acute stroke refers to the clinical pathological state caused by the acute disruption of cerebral blood vessels. It can result in either the interruption of blood supply to the brain or the rupture of brain vessels, leading to damage to brain tissue. Ischemic strokes account for about 80% of all strokes, while hemorrhagic strokes make up about 20% [4]. Ischemic stroke is caused by reduced blood flow or blockage in the cerebral vessels, leading to oxygen and blood deprivation in brain tissue. Hemorrhagic stroke results from bleeding due to the rupture of cerebral vessels, with symptoms typically appearing within minutes and potentially leading to severe neurological deficits [5].

Over the past 25 years, artificial intelligence (AI) technology has achieved remarkable progress

across various domains, notably in medical diagnostics [6]. Early AI applications primarily utilized rule-based systems and machine learning (ML) models to analyze medical data and predict outcomes. With the advent of deep learning (DL), AI's ability to handle complex medical imaging data significantly improved. DL models, such as convolutional neural networks (CNNs), have been particularly effective in automatically identifying stroke lesions and detecting stroke risk factors in medical images. These models utilize large datasets to learn intricate patterns and features, improving diagnostic accuracy and efficiency. Additionally, by integrating vast amounts of clinical data with imaging data, AI can now predict patient prognosis, assess functional recovery, and forecast treatment outcomes with greater precision [7].

The swift and precise analysis of imaging data by AI offers detailed insights into the patient's condition, significantly supporting physicians in diagnostic decision-making and treatment planning. These AI models promote a deeper understanding of disease progression, enabling the development of personalized rehabilitation plans and thereby improving long-term patient outcomes [8].

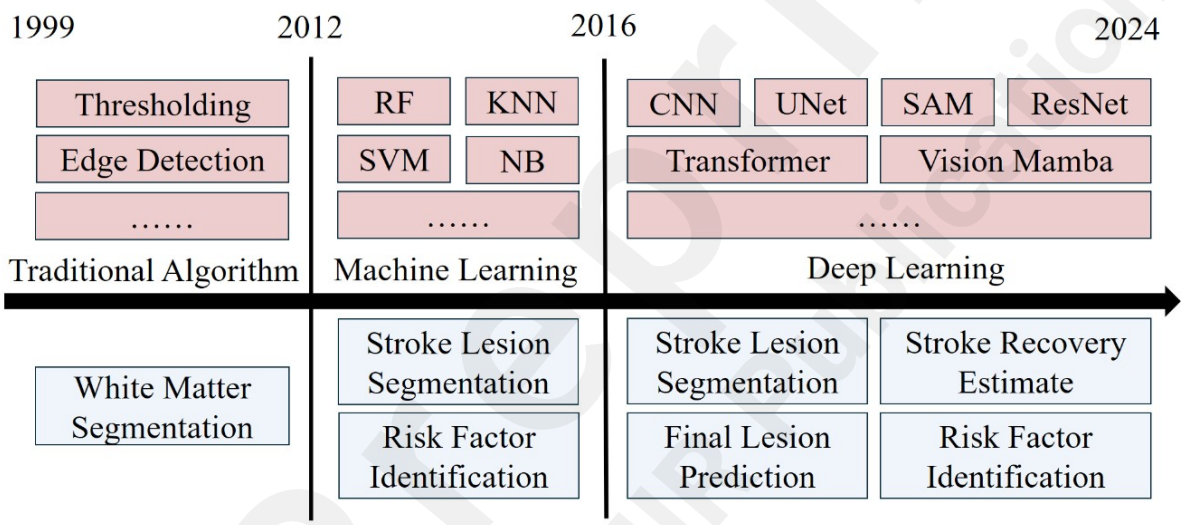

Fig.1 AI for diagnosing acute stroke over the past 25 years.

Computed Tomography (CT) and Magnetic Resonance Imaging (MRI) are the most commonly recommended imaging methods for the clinical diagnosis of acute stroke. MRI has higher clarity and clinical sensitivity, offering better soft tissue contrast [9]. MRI imaging techniques used for brain examinations include T1-weighted Imaging (T1WI), T2-weighted Imaging (T2WI), Fluid Attenuated Inversion Recovery (FLAIR), and Diffusion-Weighted Imaging (DWI), eta. T1WI provides excellent anatomical detail, but it is not very sensitive to early changes in acute stroke. T2WI can highlight increased water content in brain tissue and is commonly used for evaluating the subacute and chronic stages of stroke, although the images may be blurry and have artifacts. FLAIR can suppress cerebrospinal fluid signals, making it suitable for detecting white matter lesions and identifying lesions near the cerebrospinal fluid pathways. However, it has a longer scanning time and is not sensitive enough for detecting small infarcts. DWI is highly sensitive to early acute cerebral ischemia, but DWI images have lower resolution and are not sufficiently sensitive to small infarcts [10]. Compared to MRI imaging, CT is faster and commonly used for detecting early signs of

infarction. CT Angiography (CTA) can provide information about vascular occlusion to guide treatment decisions, while CT Perfusion Imaging (CTP) can assess the extent of ischemic core and penumbra areas [11]. The 2018 American Heart Association and American Stroke Association Guidelines (AHA/ASA 2018) indicate that non-contrast CT (NCCT) and CTA are recommended within 6 hours of acute stroke onset, while MRI and CTP are recommended for the 6 to 24-hour window [12,13]. (Fig2)

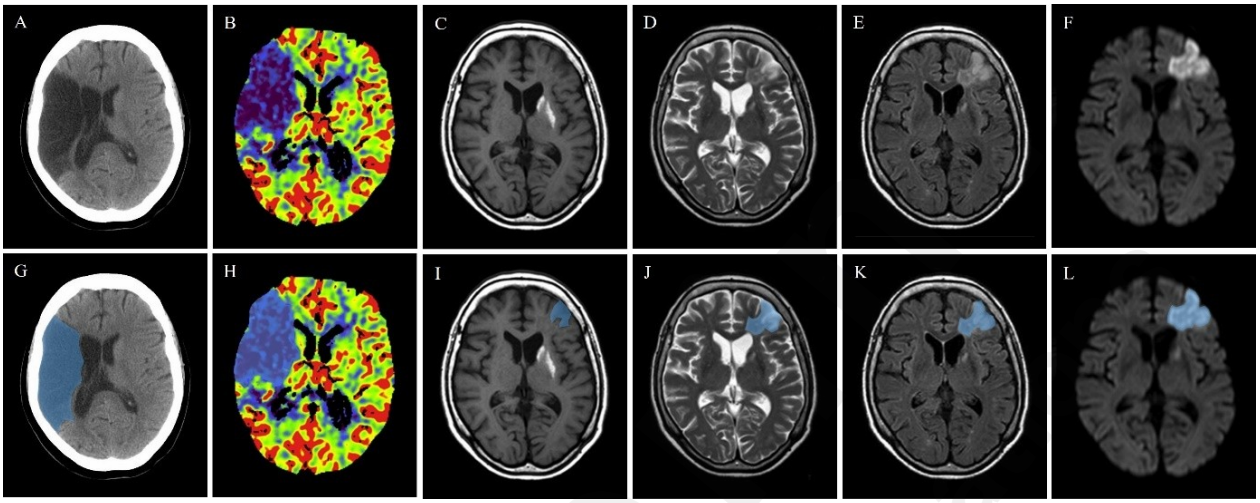

Fig.2 Stroke lesions identified using different imaging modalities. (A)NCCT; (B)CTP; (C)T1WI; (D)T2WI; (E)FLAIR; (F)DWI (G)NCCT (annotated); (H)CTP (annotated); (I)T1WI (annotated); (J)T2WI (annotated); (K)FLAIR (annotated); (L)DWI (annotated). Stroke lesion areas are marked with blue regions and the images are not paired.

Ultrasound (US) examination, with its advantages of fast imaging speed, lack of radiation, and lower cost, is commonly used in clinical practice for cardiac and carotid artery assessments [14,15]. (Fig3) For cerebral small vessel evaluation, T2WI and FLAIR weighted MRI are commonly used in clinical settings [16].

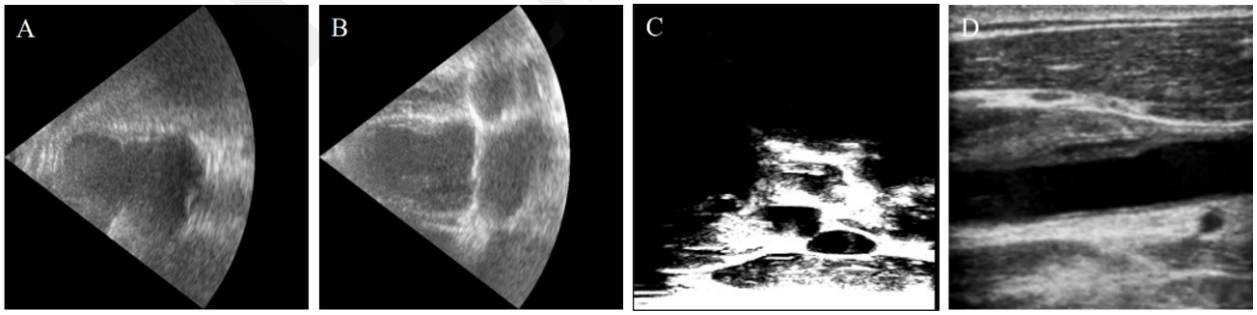

Fig.3 Cardiac US and carotid US. (A) Cardiac US (two heart chambers); (B) Cardiac US (four heart chambers); (C) 3D Carotid US; (D) 2D Carotid US.

The main contributions of this article are as follows: Firstly, this paper provides a comprehensive summary of the common applications of AI in the diagnosis of acute stroke. Secondly, this paper outlines the development trends of AI algorithms for stroke lesion segmentation

and classification, stroke risk prediction, and stroke prognosis from 1999 to 2024. It includes an analysis of data sources, types of algorithms, outcome metrics, and qualitative results described in each article. Thirdly, this paper discusses the clinical significance, existing challenges, and future research directions in this rapidly advancing field. The review aims to provide researchers and clinicians with insights into the current state of acute stroke diagnosis based on DL, offering a comprehensive reference for clinical practice.

2 Methods

For this systematic review, we adhered to the Preferred Reporting Items for Systematic reviews and Meta-Analyses (PRISMA) guideline 2020 [17]. We conducted a comprehensive literature search from January 1999 to February 2024 across multiple databases, including Google Scholar, PubMed, IEEE Xplore, Web of Science, and Springer. The Boolean search strings used were: (ABSTRACT("artificial intelligence" OR "AI" OR "machine learning" OR "deep learning" OR "CNN") AND ABSTRACT("ischemic stroke" OR "hemorrhagic stroke" OR "acute stroke" OR "stroke") AND ABSTRACT("magnetic resonance imaging" OR "MRI" OR "Computed Tomography" OR "CT" OR "Ultrasound" OR "US")).

In the initial identification phase of the PRISMA flowchart, we identified 219 articles. During the screening phase, we reviewed the titles and abstracts of these publications to remove duplicates. We also excluded articles involving animals, other lesion types (e.g., skin, lung), other stroke types (e.g., perinatal stroke, chronic stroke), and other imaging modalities (e.g., Digital Subtraction Angiography). Additionally, books, theses, review articles, and studies that did not propose an automated method based on Machine Learning (ML) or Deep Learning (DL) were excluded.

In the final inclusion phase, we retained 50 unique articles. These articles were thoroughly read to assess their eligibility for inclusion in this review. Articles were selected if they (1) relied on ML-based or DL-based automated methods and (2) included clinical medical records or medical images.

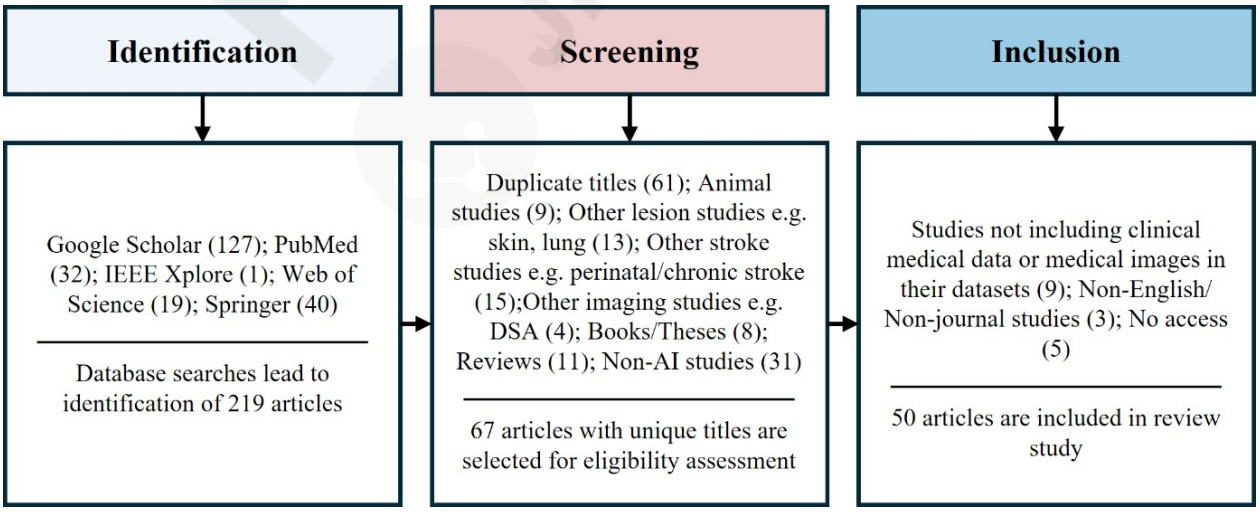

Fig.4 PRISMA flowchart for systematic filtering and selection of articles.

Table1 Acronyms with their definition.

Acronym	Definition	Acronym	Definition
AI	Artificial Intelligence	PPV	Positive Predictive Value
ML	Machine Learning	SVM	Support Vector Machines
DL	Deep Learning	RF	Random Forests
CNNs	Convolutional Neural Networks	NB	Gaussian Naive Bayes
CT	Computed Tomography	MRF	Markov Random Field
MRI	Magnetic Resonance Imaging	MHCA	Multi-Head Cross Attention
T1WI	T1-weighted Imaging	FCN	Fully Convolutional Network
T2WI	T2-weighted Imaging	DT	Decision Tree
FLAIR	Fluid Attenuated Inversion Recovery	KNN	K-Nearest Neighbors
DWI	Diffusion-Weighted Imaging	LAA	Large Artery Atherosclerosis
CTA	CT Angiography	CE	Cardioembolism
CTP	CT Perfusion Imaging	SAO	Small Artery Occlusion
NCCT	Non-contrast CT	WMH	White Matter Hyperintensities
AF	Atrial Fibrillation	LA	Left Atrium
CAS	Carotid Artery Stenosis	SE	Squeeze-and-excitation
CSVD	Cerebral Small Vessel Disease	SAM	Segment Anything Model
US	Ultrasound	VIT	Vision Transformer
DSC	Dice Similarity Coefficient	VMamba	Vision Mamba
HD	Hausdorff Distance	LLMs	Large Language Models
AUC	Area Under the Curve	ROI	Region of Interest
ACC	Accuracy	DNN	Deep Neural Network
PCA	Principal Component Analysis	RBF	Radial Basis Function
RBM	Restricted Boltzmann Machine	GRU	Gated Recurrent Unit
ASPECTS	Alberta Stroke Program Early CT Score		
STRIVE-1	Standards for Reporting Vascular Changes on Neuroimaging-1		

3 Evaluation metrics

To assist readers in gaining a clearer understanding of these articles, we will explain the model evaluation metrics featured in this review, as shown in Table 1. Common metrics include Dice Similarity Coefficient (DSC) [18], Hausdorff Distance (HD) [19], Area Under the Curve (AUC) [20], Accuracy (ACC) [21], Positive Predictive Value (PPV) [22], Recall [22], and Specificity (SPC) [22]. For image segmentation tasks, the main focus is on the DSC and HD metrics. For image classification tasks and prediction tasks, the main focus is on the ACC, PPV, Recall, SPC, and AUC metrics.

Table2 Equations and significance for evaluation metrics.

Metrics	Equations	Significance
Segmentation metrics		
DSC [18]	$2\vee X\cap Y\vee\frac{¿}{¿\,X\vee+¿\,Y}$	The overlap between segmentation results and labels.
HD [19]	$max\left(\check{H}\left(A,B\right),\check{H}\left(B,.\right.\right.$	The maximum boundary distance between results and labels.
Classification and prediction metrics		
AUC [20]		Threshold-independent classification performance.
ACC [21]	$\frac{TP+TN}{TP+TN+FP+FN}$	The proportion of correct predictions among all cases.

PPV [22]	$\frac{TP}{TP+FP}$	The proportion of true positives among predicted positives.
Recall [22]	$\frac{TP}{TP+FN}$	The proportion of true positives among all actual positives.
SPC [22]	$\frac{TN}{TP+FN}$	The proportion of true negatives among all actual negatives.

TP: True Positive; FP: False Positive; TN: True Negative; and FN: False Negative; X and Y represent the segmentation result and label, respectively; $\check{H}(A,B)$ denotes the directed Hausdorff distance from set A to set B. PPV can also be referred to as Precision. Recall can also be referred to as Sensitivity.

In this review, we also examined the statistical measures of significance and uncertainty, robustness or sensitivity analysis, methods for explainability or interpretability, and their validation, including validation or testing on external data, if reported in the studies [23].

4 Results

4.1 Segmentation and classification of stroke lesions

Imaging examinations are typically included in the admission tests for acute stroke patients [24,25]. Segmentation of stroke lesions can determine lesion volume and lesion location [26]. Classification of stroke lesions allows for the rapid identification of stroke type, aiding in patient triage [27]. This supports disease diagnosis, assists physicians in formulating treatment plans based on the patient's clinical presentation, and provides guidance for surgical or pharmacological interventions.

4.1.1 Stroke lesion segmentation based on ML

Stroke lesions segmentation is a challenging task due to the blurred boundaries between stroke lesions and normal tissues, particularly in hemorrhagic strokes. MRI images offer greater contrast and clarity compared to CT scans, allowing for more clearly delineated observation of stroke lesion boundaries [28].

Traditional thresholding and heuristic algorithms are inadequate for accurately segmenting stroke lesions. Before 2012, there was limited research on stroke lesion segmentation [29,30].

From 2012 to 2016, stroke lesion segmentation algorithms were primarily based on ML algorithms, with common segmentation methods mainly utilizing Support Vector Machines (SVM) [31], Random Forests (RF) [32], and Naive Bayes (NB) [33], eta. Due to the limited feature extraction capabilities of ML segmentation algorithms, the segmentation algorithms primarily use MRI images during this period.

In 2014, Maier et al. proposed an image segmentation method for ischemic stroke lesions based on SVM using multimodal MRI images. They used SVM to extract local features from the multimodal MRI data [34]. In the same year, Mitra et al. utilized a Bayesian-Markov Random Field (B-MRF) for preliminary FLAIR image classification, then analyzed multimodal MRI data (T1WI, T2WI, FLAIR, DWI) and contextually relevant features using a RF to identify likely lesion areas [35].

One year later, Maier et al. proposed another method for segmenting ischemic stroke lesions

in multimodal MRI images using Extra Tree forests. This approach utilized Extra Trees for voxel-level classification and incorporated intensity-derived image features [36].

In 2016, Pustina et al. proposed an automatic segmentation algorithm for stroke lesions in T1WI images, combining RF with multi-resolution neighborhood data analysis to enhance efficiency and reduce observer dependency [37]. In the same year, Griffis et al. employed a stroke lesion segmentation method based on the Gaussian Naive Bayes (GNB) classifier. By using probabilistic tissue segmentation and image algebra to create feature maps, they encoded information about missing and abnormal tissues and used the leave-one-out method for cross-validation [38].

4.1.2 Stroke lesion segmentation based on DL

After 2016, there has been a leap in the capabilities of DL for medical segmentation and feature extraction. DL has outperformed ML as the main force in stroke image segmentation [39]. Due to the improved feature extraction capabilities of DL, algorithms for stroke lesion segmentation based on CT scans have emerged.

In 2018, Goncharov et al. proposed a CNN framework integrating UNet and T-Net. In each network, convolutional layers were replaced with residual blocks and an initial convolution layer was added to enhance the learnability of the deep network [40].

In 2019, Clèrigues et al. proposed a 3D CTP segmentation method based on a 2D asymmetrical residual CNN. This method addresses issues such as small sample size, class imbalance, and overfitting by enhancing training, using symmetric modality augmentation, and applying uncertainty filtering, thereby improving performance and achieving fast inference [41].

In 2020, Wang et al. proposed a multimodal 3D CTP segmentation method based on CNNs. They extracted features from CTA images, synthesized pseudo-DWI, and used an innovative loss function to focus on lesion areas, thereby improving segmentation accuracy [42].

In 2021, Kuang et al. proposed a DL approach named EIS-Net, which combines a 3D triple CNN and a multi-region classification network for automatic segmentation of early ischemic strokes and Alberta Stroke Program Early CT Score (ASPECTS) scoring on NCCT in patients with acute ischemic stroke [43]. In the same year, Soltanpour et al. proposed an improved version of the UNet network called MultiRes UNet for the automatic segmentation of ischemic stroke lesions in CTP images. The algorithm utilizes multi-scale convolutional blocks and incorporates contralateral CT images as references, estimating lesion locations using Tmax heatmaps [44]. Luo et al. proposed an ischemic stroke lesion segmentation method called UCATR for NCCT images. This method combines ResNet-50 and Transformer encoders and introduces a Multi-Head Cross Attention (MHCA) module in the decoder to improve the accuracy of spatial information recovery [45].

In 2023, Vries et al. proposed a model called Perf-UNet for segmenting the infarct core area from CT perfusion source data. The model employs a symmetry-aware spatio-temporal convolutional structure, leveraging the dynamics of cerebral microperfusion, and incorporates attention modules in the skip connections [46].

In 2024, Kuang et al. proposed a Hybrid CNN-Transformer network based on circular feature interactions and bilateral difference learning. This network introduces a hybrid CNN-Transformer in the encoder, a recurrent feature interaction module, and a shared CNN decoder with bilateral

difference learning modules [47].

Compared to CT-based stroke lesion segmentation, MRI-based stroke lesion segmentation achieves higher segmentation accuracy.

In 2017, Chen et al. proposed a CNN network composed of a Deconvolutional Network for initial segmentation and a Multi-Scale Convolutional Label Evaluation Network for eliminating false positives in small lesions [48].

In 2018, Zhang et al. proposed FC-DenseNet for segmenting acute stroke lesions in DWI medical images. This model combines dense connections and multiscale context on top of a 3D CNN to address common issues in DWI, such as noise, artifacts, and variations in lesion size and location [49].

In 2019, Karthik et al. proposed an improved Fully Convolutional Network (FCN) that applies Leaky ReLU activation in the last two layers of the UNet architecture. This approach precisely reconstructs ischemic lesions and allows the network to learn additional features not considered in the original UNet architecture [50].

In 2020, Clèrigues et al. addressed class imbalance issues by employing symmetric modality enhancement, balanced training sample strategies, and dynamic weighted loss functions in the UNet architecture [51].

In 2023, Wu et al. introduced a lesion boundary rendering method named TransRender. This method utilizes Transformers to capture global information during the encoding phase and employs multiple renderings to effectively map encoding features of different levels to the original spatial resolution. The method adaptively selects points to compute boundary features based on point-wise rendering, supervising the rendering module to generate points and continuously refine uncertain regions [52]. In the same year, Wu et al. proposed a two-phase brain multimodal MRI lesion segmentation method named W-Net. This method utilizes CNN and Transformer as backbone networks, introduces a Boundary Deformation Module (BDM) and a Boundary Constraint Module (BCM) to address boundary ambiguity, and designs a multi-task learning loss function to optimize W-Net from both regional and boundary perspectives [53]. Soh et al. proposed an algorithm named Hybrid UNet Transformer. This algorithm comprises two parallel pipelines, where the Transformer-based pipeline utilizes feature maps from the intermediate layers of the UNet-based pipeline to enhance feature extraction capabilities [54].

4.1.3 Stroke classification

The admission evaluation for acute stroke patients typically includes stroke classification. Patients with acute ischemic stroke who are eligible for thrombolytic therapy should be referred to a thrombolytic center for treatment. For patients who are not suitable for thrombolytic therapy, conservative treatment should be provided upon admission. Hemorrhagic stroke patients require rapid intervention to minimize brain damage and improve survival chances [24].

Acute ischemic stroke classification is typically based on CT imaging [55]. In CT images, ischemic stroke lesions appear as low-density regions (dark areas), while hemorrhagic stroke lesions appear as high-density regions (white areas) [56–58].

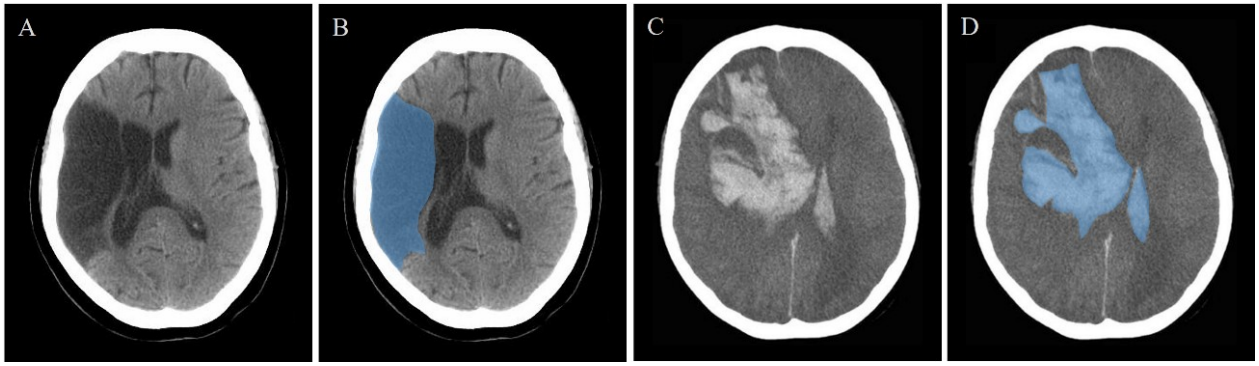

Fig.5 Ischemic stroke and hemorrhagic stroke. (A) Ischemic stroke; (B) Ischemic stroke (annotated); (C) Hemorrhagic stroke; (D) Hemorrhagic stroke (annotated). Stroke lesion areas are marked with blue regions.

Adam et al. proposed a stroke lesion classification model based on Decision Tree (DT) and K-Nearest Neighbors (KNN) algorithms. The study found that the DT algorithm outperformed KNN in classification [56].

Gautam et al. proposed a CNN model for classifying stroke CT images. They improved the quality of CT images by using a multi-focus image fusion preprocessing, and then inputted the processed images into a 13-layer CNN architecture for classification [57].

Chen et al. utilized hyperparameter optimization and transfer learning to identify stroke conditions in brain CT images. The optimized CNN and ResNet-50 models demonstrated high accuracy in distinguishing between normal, hemorrhagic stroke, ischemic stroke, and other lesions. Although ResNet-50 exhibited the highest accuracy, it required more processing time [58].

Table3 Methods and performance of stroke lesion segmentation and classification. M-MRI strand for Multimodal MRI, and M-CT strand for Multimodal CT.

Investigators	Year	Image type	Dataset	Methods	Performance	Merits
Machine learning (MRI)						
Maier et al. [34]	2014	M-MRI	36	SVM	DSC = 0.74	Use SVM to extract local features.
Mitra et al. [35]	2014	M-MRI	36	B-MRF, RF	DSC = 0.39 ± 0.22	1. Multi-stage algorithm. 2. Fuse T1WI, T2WI, FLAIR, and DWI.
Maier et al. [36]	2015	M-MRI	37	RF	DSC = 0.65 HD = 28.61 (mm)	1. Utilize Extra Trees fo classification. 2. Incorporate inten features.
Pustina et al. [37]	2016	T1WI	105	RF	DSC = 0.696 ± 0.16 HD = 17.9 ± 9.8 (mm)	Combine RF wit neighborhood data analysis.
Griffis et al. [38]	2016	T1WI	30	GNB	DSC = 0.66	1. Incorporate segmentation. 2. Incorporate image algebra.
Deep learning (CT)						
Gonchar et al. [40]	2018	vCTPet	156	all UNet	DSC = 0.53± 0.01 HD = 23.292± 0.02	1. Integrate UNet and T-Net. 2. Incorporate residual blocks.

					(mm)	
Clèrigues et al. [41]	2019	CTP	156	CNN	DSC = 0.49 ± 0.31 HD = 11.3 ± 21.6 (mm)	1. Use symmetric modality augmentation. 2. Apply uncertainty filtering.
Wang et al. [42]	2020	M-CT	156	CNN	DSC = 0.51 ± 0.31 HD = 0.55 ± 2.03 (mm)	1. Use an innovative loss function. 2. Utilize CTA to synthesize pseudo DWI.
Kuang et al. [43]	2021	NCCT	230	CNN	DSC = 0.448	1. Combine CNN and classification network. 2. Introduce the ASPECTS scale.
Soltanpour et al. [44]	2021	CTP	156	UNet	DSC = 0.69	1. Utilize multi-scale convolutional blocks. 2. Incorporate contralateral CT images. 3. Use Tmax heatmaps.
Luo et al. [45]	2021	NCCT	293	Transformer, Resnet-50	DSC = 0.7358	1. Combine ResNet-50 and Transformer. 2. Introduce Multi-Head Cross Attention.
Vries et al. [46]	2023	CTP	156	UNet	DSC = 0.564	1. Incorporate symmetric temporal. 2. Use the dynamic microperfusion. 3. Incorporate attention in skip connections.

Kuang et al. [47]	2024	NCCT	482	Transformer, CNN	DSC = 0.5407	1. Introduce hybrid CNN-Transformer. 2. Introduce bilateral difference learning.
Deep learning (MRI)						
Chen et al. [48]	2017	DWI	741	CNN	DSC = 0.67	1. Multi-stage algorithm. 2. Introduce multi-scale concept.
Zhang et al. [49]	2018	DWI	242	DenseNet	DSC = 0.7913	Combine dense connections and multiscale context.
Karthik et al. [50]	2019	MMRI	28	FCN	DSC = 0.70	Use Leaky ReLU in last two layers.
Clèrigues et al. [51]	2020	MMRI	236	UNet	DSC = 0.59± 0.31 HD = 0.84± 0.10 (mm)	1. Employ symmetric modality enhancement. 2. Use dynamic weighted loss functions.
Wu et al. [52]	2023	MMRI	490	Transformer	DSC = 0.7258	Use point-wise render boundary.
Wu et al. [53]	2023	MMRI	490	Transformer, CNN	DSC = 0.7368	1. Multi-stage algorithm. 2. Propose two edge enhancement modules.
Soh et al. [54]	2023	T1WI	239	Transformer, UNet	DSC = 0.737	Comprise two parallel pipelines.
Stroke classification						
Adam et al. [56]	2016	NCCT	400	DT, CNN	AUC = 0.994 Recall = 0.987	Compare KNN and DT.
Gautam et al. [57]	2021	NCCT	900	CNN	ACC = 98.33	Use a multi-fo

						preprocessing.
Chen et al. [58]	2022	NCCT	400	CNN	Recall = 0.99	1. Use hyperparameter optimization. 2. Use transfer learning. 3. Compare optimized CNN and ResNet-50.

4.1.4 Discussion of stroke lesion segmentation and classification

In clinical practice, the choice between MRI and CT depends on the specific condition of the patient. CT has lower sensitivity in identifying early changes of acute ischemic stroke but demonstrates higher sensitivity in detecting characteristic high-density lesions of hemorrhagic stroke [59]. Compared to CT, MRI has higher contrast and a stronger ability to differentiate between brain tissues. The DWI sequence can detect minor changes in brain tissue just minutes after ischemia occurs. MRI also provides clearer identification of small hemorrhages and better differentiation between hemorrhage and ischemic areas, along with detailed information on the extent and type of brain tissue damage following a stroke [60].

Before 2012, brain segmentation algorithms were primarily based on traditional methods for brain white matter segmentation. There are few studies focusing on the segmentation of stroke lesions in this period [29,30]. Between 2012 and 2016, segmentation algorithms for ischemic stroke lesions were primarily based on ML. Due to the blurred boundaries between stroke lesions and surrounding normal tissue in CT images, algorithms from this period mainly focused on MRI imaging. The accuracy of segmentation algorithms during this time generally did not exceed 0.75. These algorithms were complex, have weak generalization capabilities, and could not achieve the level of accuracy of manual segmentation. After 2016, with the development of UNet, DL has shown superior performance in the segmentation of stroke lesions [39]. DL enables more in-depth feature extraction from medical images, significantly enhancing the extraction of effective features, an increasing number of researchers have started focusing on the segmentation of ischemic stroke lesions in CT images. However, the accuracy of these segmentation algorithms based on CT commonly did not surpass 0.75. Algorithms for segmenting ischemic stroke lesions based on MRI have shown better accuracy, enough to be comparable to manual segmentation. Some algorithms have achieved accuracies up to 0.85. To facilitate the triage of patients with acute stroke, due to the urgency of the condition, classification of stroke types primarily relies on CT images [55]. Current algorithms had achieved high accuracies, generally exceeding 0.9, indicating

promising application prospects.

Data preprocessing is important for medical image segmentation. Preprocessing aims to standardize image quality, enhance valuable features, and reduce segmentation difficulties. References [41,51] employed symmetry-enhanced modalities, leveraging the high bilateral symmetry exhibited by the human brain in its natural state. This approach provides clearer and more accurate information for subsequent steps such as feature extraction, lesion detection, and image segmentation. For complex segmentation tasks such as stroke lesion segmentation, the introduction of multimodal approaches can significantly enhance algorithm performance by extracting complementary information from different imaging techniques. References [35,42] are particularly representative. Reference [35] employs multimodal MRI data including T1WI, T2WI, FLAIR, and DWI, along with context-aware features. Reference [42] extracts feature from CTA images and synthesizes pseudo-DWI for use in CTP segmentation methods.

Additionally, some studies have employed multi-stage algorithms, combining coarse and fine-grained approaches to achieve better segmentation performance. For instance, reference [35] uses a B-MRF model for preliminary classification of FLAIR images and employs RF for multimodal MRI segmentation. Reference [48] utilizes a Deconvolutional Network for initial segmentation and employs a Multi-Scale Convolutional Label Evaluation Network to evaluate and eliminate false positives of small lesions, achieving promising results on large datasets and demonstrating the algorithm's generalization ability.

Since 2021, various attention mechanisms and Transformers have been widely applied in the field of medical image segmentation, leading to further improvements in the performance of stroke lesion segmentation algorithms. Transformers leverage self-attention mechanisms, enabling neural networks to capture global information and exhibit excellent performance when processing long sequence data [61]. Reference [46] introduces attention mechanisms on the skip connections between the encoder and decoder, reducing the time dimension and only propagating the most informative features. References [45,47,52–54] all incorporate the

concept of Transformers, leading to significant improvements in algorithm performance.

4.2 Stroke risk prediction

Clinical methods for stroke risk prediction include clinical risk scores (e.g., Framingham Stroke Risk Profile [62]), genetic risk analysis [63], serum biomarker detection [64], and imaging analysis [65]. Compared to other methods, imaging analysis provide direct anatomical and functional information, allowing clinicians to observe pathological conditions directly. Additionally, imaging data can quantify stroke risk factors such as atrial fibrillation (AF), carotid artery stenosis (CAS), and cerebral small vessel disease (CSVD), which are crucial for stroke risk prediction [66]. Furthermore, imaging techniques can monitor disease progression and treatment effects in real-time, enabling clinicians to adjust treatment strategies promptly. Due to these advantages of imaging techniques, AI-based stroke risk prediction using medical imaging has become a major focus of research.

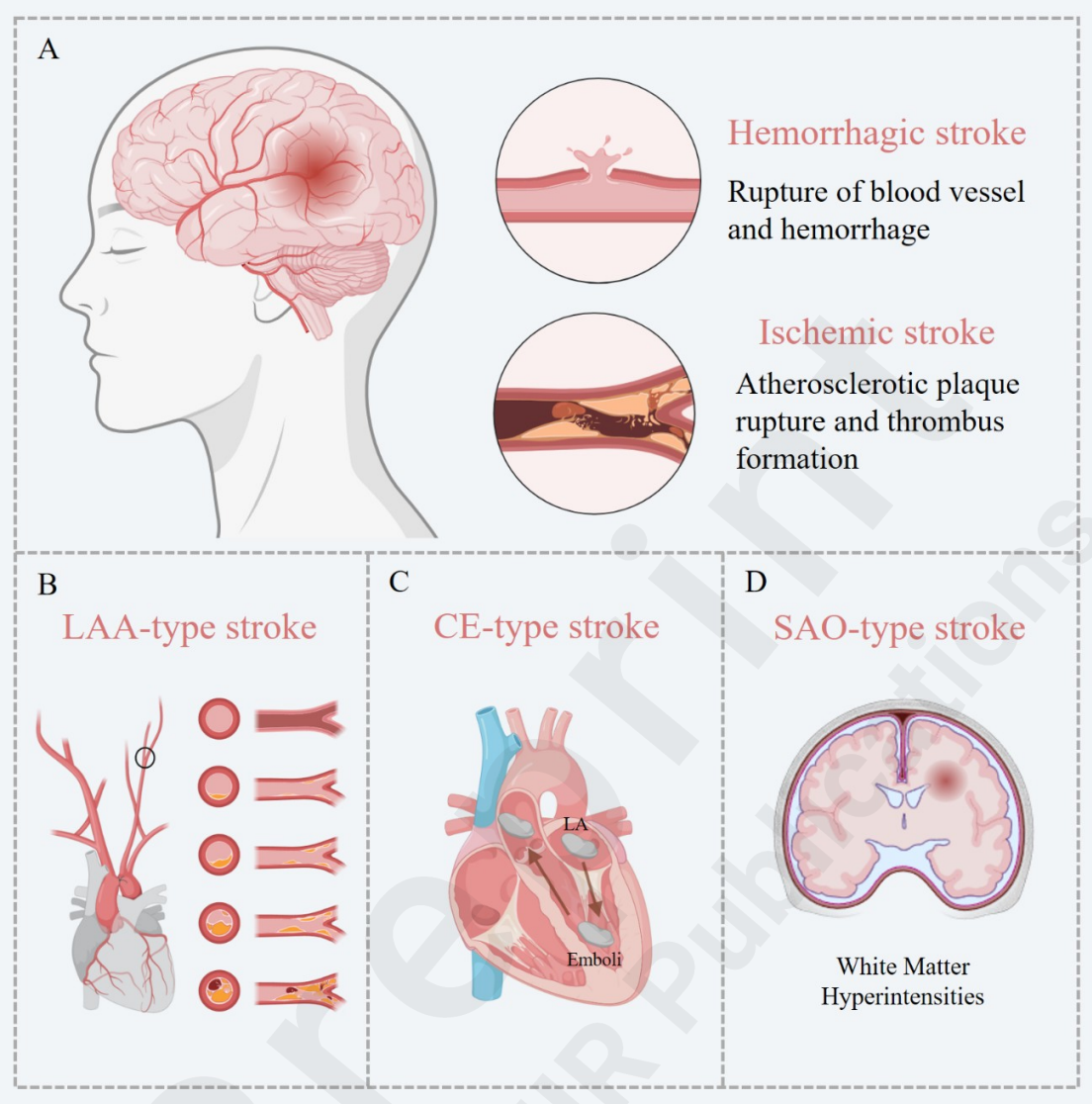

Fig.6 Risk factors and etiology of stroke. (A) Hemorrhagic stroke and Ischemic stroke; (B) LAA-type stroke and its risk factors; (C) CE-type stroke and its risk factors; (D) SAO-type stroke and its risk factors.

4.2.1 Risk factors of stroke

Stroke can be divided into three distinct subtypes with well-defined etiologies: large artery atherosclerosis (LAA), cardioembolism (CE), and small artery occlusion (SAO) [66].

LAA-type stroke is typically caused by atherosclerotic stenosis in the carotid and intracranial large arteries. For patients with mild stenosis, conservative treatment is

recommended. For those with severe stenosis, carotid endarterectomy surgery is performed to prevent the occurrence of ischemic stroke [67].

CE-type stroke is caused by cardiogenic diseases, where emboli from the heart and aortic arch dislodge and circulate, leading to cerebral artery embolism [68]. Studies have shown that left atrial (LA) enlargement may lead to myocardial fibrosis and disruption of atrial muscle bundles, resulting in blood stasis within the atrium and reduced atrial contraction capacity. This can lead to AF, thereby increasing the risk of cardioembolic stroke [69].

SAO-type stroke, also known as lacunar stroke, is a pathological condition caused by the disease of small penetrating arteries in the deep regions of the cerebral hemispheres or brainstem, leading to ischemic necrosis of the brain tissue supplied by these arteries [70]. The international neuroimaging standard STRIVE-1 (Standards for Reporting Vascular Changes on Neuroimaging-1) clearly states that white matter hyperintensities (WMH) are neuroimaging indicators of small vessel disease and can predict the occurrence of stroke [16].

4.2.2 AI-assisted detection of CAS

The most commonly used imaging method for the detection of CAS in clinical practice is US [71,72].

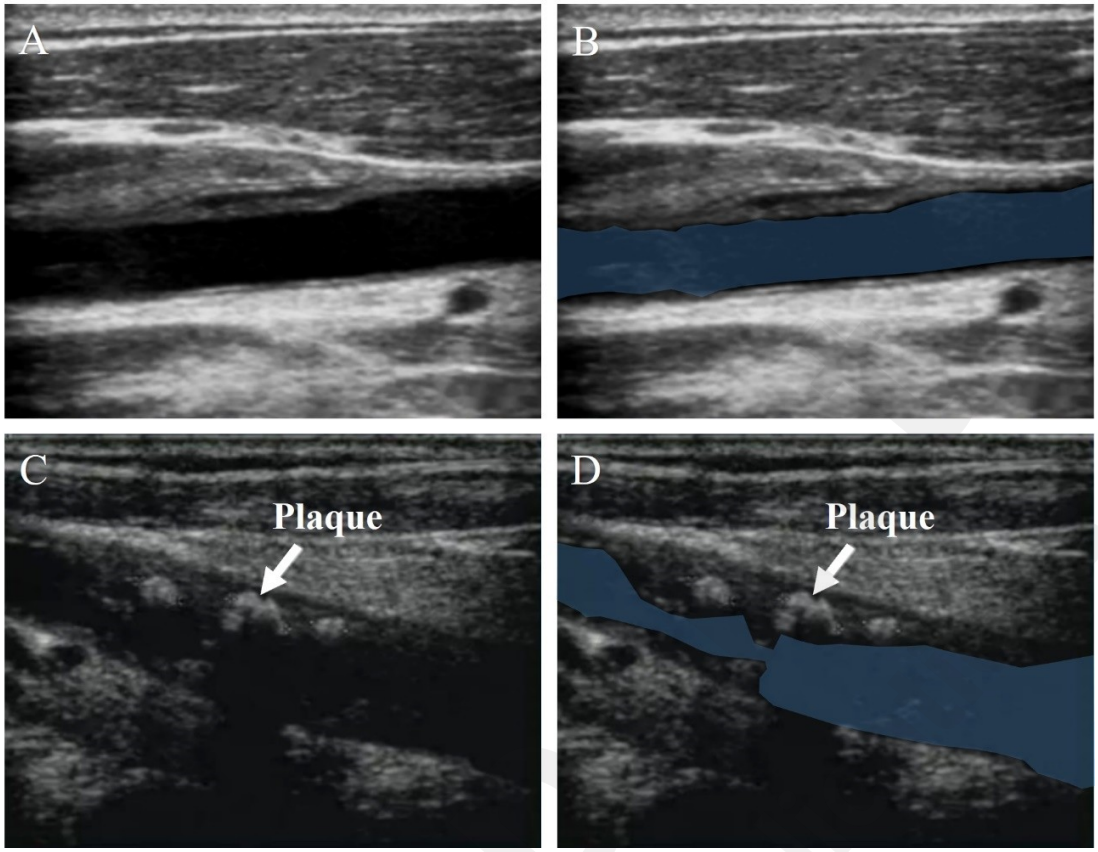

Fig.7 Carotid artery stenosis. (A) Health people; (B) Health people (annotated); (C) Patient with CAS; (D) Patient with CAS (annotated). Lumens are marked with blue regions.

In 2015, Alam et al. proposed a Robust Fuzzy Radial Basis Function Network that combines Fuzzy C-Means clustering and Radial Basis Function Network, incorporating spatial information and a smoothing parameter to handle noise [73].

In 2017, Araki et al. combined improved spatial domain filtering techniques with ML to utilize the morphological differences in carotid artery walls from US images. They used the improved spatial domain filtering techniques to remove image noise and employed SVM for classification [74].

In 2021, Al-Mohannadi et al. introduced morphological operations in an encoder-decoder structure to reduce the impact of noise on the results, using Sobel gradient direction images and Prewitt gradient direction images as inputs [75]. In the same year, Mi et al. designed an MBFF-Net with three branches. The first two branches extract plaque features at

multiple scales and different contexts, while the other branch utilizes prior information [76].

In 2022, Latha et al. compared various ML and DL algorithms in the task of carotid artery segmentation. Among the ML algorithms, RF performed the best, while CapsuleNet outperformed other DL algorithms [77].

In 2023, Jiang et al. integrated a centerline extraction network and a dual-stream centerline-guided network into a 3D UNet. The centerline extraction network generates centerline heatmaps to indicate the position of the carotid artery centerline, while the centerline-guided network segments the 3D US images based on the centerline heatmaps [78].

4.2.3 AI-assisted detection of AF and LA enlargement

Similar to CAS, echocardiography is commonly used clinically to detect stroke-related heart disease, such as AF and LA enlargement [15].

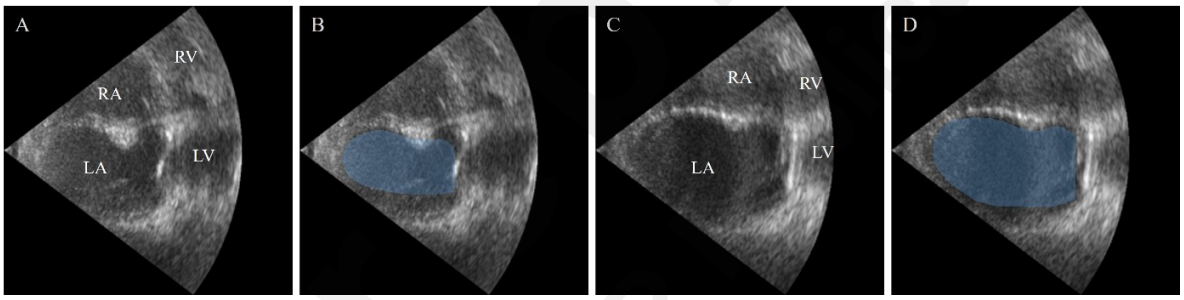

Fig.8 The presence of LA enlargement. (A) Health people; (B) Health people (annotated); (C) Patient with LA enlargement; (D) Patient with LA enlargement (annotated). LA areas are marked with blue regions.

In 2018, Degel et al. proposed an algorithm that combines DL, shape priors, and adversarial learning to achieve automatic segmentation of the LA in 3D US images. This algorithm uses V-Net for 3D volume segmentation and trains an autoencoder network to constrain the segmentation results to the shape of the LA [79].

In 2019, Moradi et al. proposed MFP-UNet, which combines a pyramid network with the UNet model, adding two downsampling layers to extract more detailed features from the images. They also used Niblack's global thresholding method to preprocess the cardiac US

images to enhance contrast [80].

In 2020, Leclerc et al. proposed an RUNet composed of two UNets. The first UNet obtains the Region of Interest (ROI) by dilating the preliminary results, and the second UNet is used to predict the final segmentation. RUNet outperformed other networks in reducing geometric and anatomical prediction anomalies [81].

In 2021, Liu et al. introduced a pyramid-shaped local attention mechanism in UNet to capture contextual information and designed a label consistency learning mechanism to improve the classification accuracy of edge pixels in cardiac US images [82].

In 2023, Li et al. proposed a multi-task DL model for cardiac US segmentation and key point detection, named EchoEFNet. The network introduces residual networks, branched networks, and dilated convolutions in the encoder part, and incorporates multi-scale concepts in the decoder part, combining both low-level and high-level features [83].

4.2.4 AI-assisted detection of WMH

MRI is superior to CT in terms of soft tissue contrast, allowing for better differentiation between white matter and gray matter in the brain. Therefore, MRI is more commonly used clinically to detect CSVD and WMH [84,85].

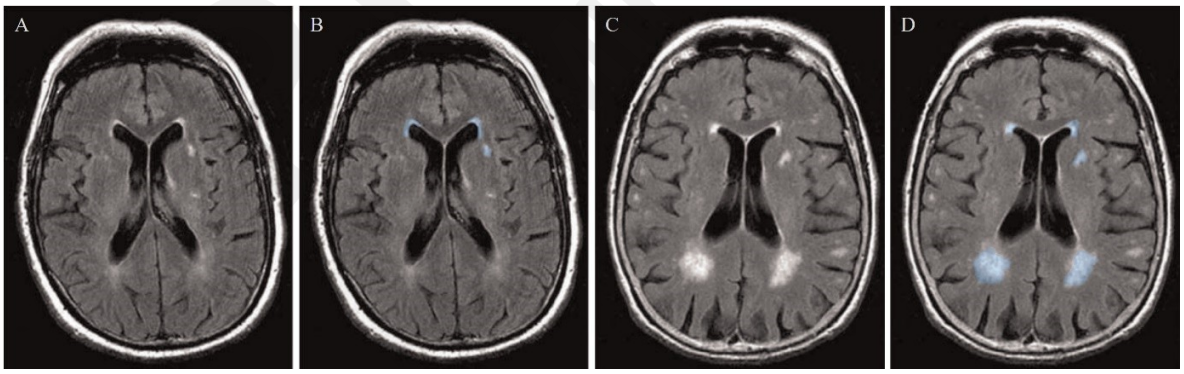

Fig.9 The presence of WMH. (A) Patient with minor WMH; (B) Patient with minor WMH (annotated); (C) Patient with extensive WMH; (D) Patient with extensive WMH (annotated). WMH areas are marked with blue regions.

In 2020, Liu et al. proposed the M2DCNN, a network composed of two symmetrical

U-shaped subnetworks. This network utilizes dense blocks, dilated blocks, and multi-scale processing to improve feature extraction and prediction capabilities. Additionally, it introduces a loss function based on the similarity between lesions and background [86].

In 2021, Park et al. proposed a UNet with multi-scale foreground highlighting, incorporating an auxiliary classifier in the middle layers of the decoder for deep supervision training. They used multi-scale label images and applied the Highlight Foreground method to enhance foreground voxels [87].

In 2021, Li et al. introduced squeeze-and-excitation (SE) blocks and dense connections into the UNet architecture to better capture spatial and multi-scale semantic information [88].

In 2023, Huang et al. proposed the LSLoss loss function. LSLoss consists of four loss terms, each designed to optimize foreground loss, background loss, ROI loss, and divergence loss, to improve the accuracy of segmentation results [89].

In 2024, Farkhani et al. proposed the VoSHT architecture, which enhances the UNet by using consecutive self-attention encoders to capture spatial dependencies in the data [90].

Table4 Methods and performance of stroke prediction.

Investigators	Year	Image type	Dataset	Methods	Performance	Merits
AI-assisted detection of CAS						
Alam et al. [73]	2015	US	200	RBF	ACC = 0.982	1. Combine Fuzzy C-Means clustering. 2. Incorporate noise handling methods.
Araki et al. [74]	2017	US	407	SVM	ACC = 0.9428	Use spatial domain filtering.
Al-Mohannadi et al. [75]	2021	US	100	Encoder-decoder	DSC = 0.7423	Introduce edge operators.
Mi et al. [76]	2021	US	430	UNet	DSC = 0.780	1. Designed a three-branch network 2. Utilize the prior knowledge of carc artery.
Latha et al. [67]	2022	US	361	CapsuleNet	ACC = 0.967	Compare multiple DL and ML models.
Jiang et al. [78]	2023	US	244	CNN	DSC = 0.927 ± 0.054	Introduce the conc extraction.
AI-assisted detection of AF and LA enlargement						
Degel et al. [79]	2018	US	161	CNN	DSC = 0.75 ± 0.17 HD = 4.46 ± 2.27 (mm)	1. Introduce shape prior. 2. Introduce adversarial learning.
Moradi et al. [80]	2019	US	1137	UNet	DSC = 0.945 ± 0.12 HD = 1.62 ± 2.0 (mm)	1. Combine a pyramid network with UNet. 2. Use Otsu's global thresholding.

					(mm)	
Leclerc et al. [81]	2020	US	2000	UNet	HD = 5.9 ±3.6 (mm)	1. Cascaded Network. 2. Present a novel attention mechanism.
Liu et al. [82]	2021	US	3500	UNet	DSC = 0.949 HD = 4.33 (mm)	1. Propose a pyramid local attention module. 2. Propose a label coheren mechanism.
Li et al. [83]	2023	US	1764	ResNet	DSC = 0.959 ± 0.002 HD = 0.422 ± 0.314 (mm)	1. Introduce resid networks. 2. Introduce dilated convolutions. 3. Incorporate multi-scale concepts in decoder.
AI-assisted detection of WMH						
Liu et al. [86]	2020	MRI	75	CNN	DSC = 93.49	1. Cascaded Network. 2. Utilize dense blocks, dilated blocks. 3. Utilize multi-scale processing.
Park et al. [87]	2021	MRI	170	UNet	DSC = 0.718 ± 0.0203	1. Incorporate an auxiliary classifier. 2. Apply the Highlight Foreground method. 3. Utilize multimodal MRI images.
Li et al. [88]	2021	MRI	40	UNet	DSC = 0.736 ± 0.074	Introduce SE blocks and dense connection.
Huang et al. [89]	2023	MRI	455	VNet	DSC = 0.81 ± 0.06	Propose the LSLoss loss function.

Farkhani et al. [90]	2024	MRI	430	UNet	DSC = 0.8559	Incorporate co encoders.

4.2.5 Discussion of stroke risk prediction

Carotid and cardiac US segmentation can assist physicians in quantitatively assessing the condition of a patient's heart and carotid arteries, providing important references for evaluating the risk of stroke. However, US image segmentation is a complex task. Compared to CT and MRI, US images have lower contrast, noisy and blurry boundaries, and numerous artifacts, making US medical image segmentation more challenging.

For US image segmentation and classification, DL generally outperforms ML. Among ML algorithms, RF performs the best in handling the tasks of segmentation and classification of US images, with high accuracy and robustness, and the ability to handle multi-feature data. In contrast, other ML algorithms like SVM and KNN perform well in certain specific tasks but are generally not as stable and accurate as RF. This is similar to the excellent performance of RF in stroke lesion segmentation and classification as discussed in Section 4.1, further demonstrating RF's superior performance in image segmentation and classification tasks [77].

To address the significant noise in US images, many researchers have incorporated denoising techniques into their algorithms. Reference [73] introduced spatial information and smoothing parameters to handle noise, and reference [74] employed spatial filtering techniques. Additionally, due to the high noise and blurry boundaries in US images, advanced architectures such as transformers may not necessarily outperform traditional convolutional blocks. In the comparative experiments in reference [82], traditional architectures like UNet, UNet++, and ResNet performed better than Swin-Unet. Although Swin-Unet, with its advanced Transformer architecture, significantly improved feature extraction and generalization capabilities, it exhibited overfitting in the segmentation of edge regions due to the substantial noise and blurred edges in US images.

The structures of carotid and cardiac US are relatively fixed, and the introduction of morphological operations can better optimize these fixed structures. This effectively reduces the impact of noise and small artifacts, improves segmentation accuracy, enhances structural features, and increases robustness. Reference [74] utilized the morphological characteristics

of the carotid artery wall to specifically improve spatial filtering, while reference [75] introduced Sobel and Prewitt operators to make the model more attentive to edge information, aiding in the identification and segmentation of the boundaries of the carotid artery and the heart. References [76,79] all incorporated shape prior information, and reference [82] introduced a label consistency learning mechanism. These four papers used the concept of templates to constrain the segmentation results and reduce missegmentation. For the segmentation of carotid vessels, centerline extraction can accurately determine the center position of the vessels, providing precise references for subsequent segmentation and feature extraction. This can largely ignore small noise and artifacts in the image, providing more stable segmentation results [78].

For WMH segmentation, many researchers have attempted to use attention mechanisms to enhance the model's focus on small targets. The attention mechanism allows the model to selectively focus on important regions of the image based on the task requirements, reducing dependence on irrelevant information [86]. Reference [90] achieved precise capture of key regions through self-attention and hybrid Transformer mechanisms, contributing to the improvement of WMH segmentation accuracy.

In the task of WMH segmentation, there is a significant class imbalance due to the large difference in the number of pixels between white matter and non-white matter regions. The model tends to predict the more numerous classes while ignoring the minority classes, leading to overfitting. To address this issue, references [86,88] introduced dense blocks, which reduce the number of training parameters and alleviate the problem of vanishing gradients.

For small target segmentation, optimizing the loss function is a promising approach. In reference [89], a level set loss function (LSLoss) was proposed to train the segmentation network. This method allows for training without actual ground truth labels, helping to avoid overfitting the training data.

4.3 Stroke prognosis

Stroke prognosis refers to predicting long-term outcomes such as recovery status,

quality of life, and survival rates of patients based on medical imaging and clinical dates. AI technology can quantify the extent of brain tissue damage, assess patients' prognostic situations, and provide benchmarks for long-term rehabilitation [91].

4.3.1 Estimation of final infarct lesion and penumbra

Acute stroke lesions tend to increase in size over time, leading to increased damage to brain tissue. To address this issue, some researchers have used AI to predict the final infarct lesions and the penumbra [92].

In 2017, McKinley et al. proposed a RF-based algorithm for penumbra prediction in multi-modal MRI, called FASTER. This algorithm first extracts various statistical metrics from perfusion and diffusion imaging in the MRI data, and then uses a decision forest algorithm to predict the penumbra [93].

In 2018, Nielsen et al. utilized CNNdeep to predict final infarct lesion, outperforming traditional General Linear Models, CNNs based on Tmax, and Apparent Diffusion Coefficient threshold methods [94].

In 2020, Yu et al. proposed a UNet-based model for predicting the final infarct lesions in patients with acute ischemic stroke. This model is the first DL-based stroke infarct prediction model that does not rely on reperfusion information, the volume error between the predicted results and the ground truth is only 9 mm^3 [95].

In 2021, Pinto et al. proposed a method combining Restricted Boltzmann Machine (RBM) and Gated Recurrent Unit (GRU) to predict the final stroke lesion in patients with acute ischemic stroke after 90 days. Each RBM learns features from different MRI parameter maps, which are then merged with the original maps and input into a convolutional and recurrent neural network architecture for supervised learning [96].

In 2022, Kelvin et al. developed a DL-based method for predicting the final infarct volume from MRI. This approach utilizes networks with rotation and reflection variants and incorporates clinical variables to predict the 90-day modified Rankin Scale score [97].

4.3.2 Estimation of stroke recovery outcomes

Clinical dates can assist in estimating stroke recovery. Lesion volume and lesion location

are critical factors in predicting recovery. Patients with extensive brain damage or strokes affecting critical brain areas generally have a poorer prognosis. Integrating patient clinical records with medical imaging can enhance the estimation of recovery outcomes [98].

Bentley et al. utilized SVM to predict whether acute ischemic stroke patients would develop symptomatic intracerebral hemorrhage after thrombolysis. Through the analysis of clinical records and brain CT images of 116 acute stroke patients, they found that SVM outperformed traditional prediction scoring systems in predicting symptomatic intracerebral hemorrhage [99].

Monteiro et al. investigated the use of ML methods to predict functional recovery in ischemic stroke patients three months after the event. The study examined the performance of five different classifiers, among which RF exhibited the best performance [100].

Cheon et al. constructed a Deep Neural Network (DNN) model combined with Principal Component Analysis (PCA) for feature extraction. The model demonstrated high predictive ability based on medical records from 15,099 stroke patients [101].

Kuang et al. proposed an automated method for ASPECTS scoring from NCCT images of patients with acute ischemic stroke. This method utilizes texture features to train an RF classifier and performs well in identifying large areas of early infarction [102].

Scrutinio et al. utilized a RF algorithm enhanced with Synthetic Minority Over-sampling Technique to predict the 3-year mortality rate of patients with severe stroke, significantly outperforming the Logistic Regression model [103].

Brugnara et al. integrated clinical records, multimodal imaging, and angiographic features to predict the modified Rankin Scale outcomes of patients with acute ischemic stroke after endovascular treatment. With the increase in medical information modalities, the model performance gradually improves [104].

Table5 Methods and performance of stroke prognosis. CR stands for clinical records.

Investigators	Year	Image type	Dataset	Methods	Performance	Merits
Estimation of final infarct lesion and penumbra						
McKinley et al. [93]	2017	MRI	80	RF	AUC = 0.94 ± 0.08	1. Automated method to estir penumbra. 2. Utilized multimodal MRI images.
Nielsen et al. [94]	2018	MRI	222	CNN	AUC = 0.88 ± 0.12	1. Integrate Tmax. 2. Use Apparent Diffusi threshold.
Yu et al. [95]	2020	MRI	182	UNet	AUC = 0.92 DSC = 0.58	Does not depend on reperfusion information.
Pinto et al. [96]	2021	MRI	75	CNN	DSC = 0.38 HD = 29.21 (mm)	1. Account the underlying cerebral l flow. 2. Combine RBM and GRU.
Kelvin et al. [97]	2022	MRI	100	UNet	DSC = 0.88 ± 0.01 ACC = 0.75 ± 0.03 AUC = 0.80 ± 0.03	1. Incorporate rotatio variants. 2. Incorporate clinical indicators. 3. Predict the modified outcomes.

Estimation of stroke recovery outcomes						
Bentley et al. [98]	2014	CT, CR	116	SVM	AUC = 0.744	Multimodal clinical records.
Monteiro et al. [99]	2018	CR	541	RF	AUC = 0.808 ± 0.085	Compare RF, XGBoost Regression.
Cheon et al. [100]	2019	CR	15099	DNN	AUC = 0.8348	Incorporate PCA into the DNN.
Kuang et al. [101]	2019	CT	257	RF	AUC = 0.89	Introduce the ASPECTS scale.
Scrutinio et al. [102]	2020	CR	1207	RF	AUC = 0.928 ACC = 0.863	Implement the synthetic mi sampling technique
Brugnara et al. [104]	2020	CT, CR	246	ML	AUC = 0.856 ACC = 0.804	1. Integrated multimodal clinical records. 2. Predict the modified outcomes.

4.3.3 Discussion of stroke prognosis

For stroke prognosis, both DL and ML have their respective advantages [105]. DL models require large amounts of data for training to learn sufficiently complex features and avoid overfitting. This also explains why the DNN in [101] achieved better performance after being trained on 15,099 medical records, while acquiring a large amount of high-quality clinical data for stroke prognosis may be challenging.

In contrast, traditional ML methods have demonstrated greater robustness and efficiency in handling stroke prognosis tasks. Studies have shown that when handling stroke prognosis tasks, RF and its variant models have shown better performance compared to other ML algorithms [100,102,103]. This is mainly due to the robustness of RF models to data noise.

For estimation of final infarct lesion and penumbra, although the existing estimation may not achieve high DSC, metrics such as volume error and AUC have reached high levels, indicating good practical value. In the future, through continuous optimization and improvement of algorithms, the clinical translation prospects of AI in final infarct estimation will be even broader.

5 Discussion

Over the past 25 years, significant advancements have been made in AI-assisted stroke diagnosis. From 1999 and 2012, development was constrained by the limited performance of traditional thresholding and heuristic algorithms, resulting in low diagnostic accuracy and restricted clinical applicability. From 2012 to 2016, the advent and advancement of ML algorithms significantly expanded research in AI-assisted stroke diagnosis. The implementation of advanced statistical models and classifiers enabled more detailed analysis of stroke imaging data and improved diagnostic precision. After 2016, DL techniques, particularly CNNs, demonstrating significant improvements over traditional methods and ML algorithms [106].

AI has significantly enhanced the accuracy and efficiency of stroke lesion segmentation and classification, stroke risk prediction (e.g., assessment of LA enlargement, CAS, and WMH), and stroke prognosis (e.g., prediction of stroke recovery outcomes, final infarct lesion, and penumbra). Stroke lesion segmentation and classification enable more precise diagnoses, reduce the time to diagnosis, and improve patient treatment outcomes. Stroke risk prediction allows for timely intervention, potentially reducing stroke occurrence. Stroke prognosis helps doctors develop personalized rehabilitation plans, optimize treatment strategies in real-time, and provide more accurate prognostic information to patients and their families. Integrating AI into clinical practice enables healthcare providers to use advanced data analysis and pattern recognition capabilities to streamline workflows, reduce diagnostic errors, enhance the diagnostic process, and improve continuous monitoring and management of stroke patients [107].

Despite the advancements described above, several challenges remain in clinical applications. Firstly, stroke diagnosis is a complex process that requires the integration of multimodal information (e.g., medical imaging, genomic data, and clinical records) for comprehensive evaluation. However, the effective integration of multimodal data with diverse formats is challenging. Secondly, AI algorithms lack effective clinical validation. The generalization ability of AI models is limited, with many algorithms performing inconsistently across different datasets and imaging devices. Additionally, AI algorithms often exhibit a "black box" nature. Therefore, it is essential to develop transparent and interpretable models to help clinicians build trust in AI-assisted diagnosis. Thirdly, the use of AI in stroke diagnosis presents privacy and data security issues. Traditional data sharing and model training methods may lead to information leakage.

Recently, the emergence of models such as Segment Anything Model (SAM) [108], Vision Mamba (VMamba) [109], and multimodal large language models (LLMs) [110] has provided new directions for stroke diagnosis. SAM boasts a large parameter count and introduces pre-trained weights from Vision Transformer (VIT), resulting in excellent

generalization performance for medical image segmentation [108]. MedSAM, a fine-tuned version of the original SAM tailored for medical images, shows a 22.51% improvement in DSC on zero-shot medical image segmentation tasks compared to the un-tuned SAM [111]. nnSAM integrates pre-trained SAM encoders and UNet encoders in parallel, combining robust feature extraction capabilities with better adaptability to different image segmentation tasks [112]. SAM performs well on external datasets from various imaging devices without further training, demonstrating potential to address the issue of limited generalization ability.

Multimodal LLMs can effectively integrate multimodal clinical data, enabling a more comprehensive understanding of patient conditions [113,114]. Gu et al. utilized LLMs for stroke quantitative evaluation using multimodal data, achieving a consistency of 0.823 with expert ratings, demonstrating outstanding performance and application prospects [115]. Recently, VMamba represents a further improvement and upgrade of the Transformer architecture. It can capture global information while maintaining linear computational complexity, addressing the performance bottleneck caused by the quadratic computational complexity of Transformers [109]. Whether VMamba can achieve a leap in performance for stroke diagnosis similar to Transformers remains to be seen and will require further evaluation over time.

Federated learning is able to address data privacy and security issues, allowing different institutions to collaboratively train AI models without sharing raw data. Federated learning not only protects patient privacy but also facilitates cross-institutional data sharing and collaboration, improving the generalization ability and accuracy of the models [116].

Overall, standardization is a key factor in promoting the application of AI in the medical field. It is necessary to establish unified evaluation standards and operational procedures to ensure that different institutions and researchers can consistently utilize AI technologies. Additionally, medical professionals need continuous education and training on AI to better understand and trust the technology, thereby applying it more effectively in clinical practice [117].

6 Conclusion

This article reviewed the current status, challenges, and development trends of AI in acute stroke lesion segmentation and classification, stroke risk prediction, and stroke prognosis over the past 25 years. AI-assisted stroke diagnosis has now shown good performance, assisting physicians in making rapid diagnoses and improving patient outcomes. With the development of new AI technologies such as SAM, LLMs, and VMamba, AI-assisted diagnosis of acute stroke will have higher accuracy and stability in the future.

Reference

1. Tu W-J, Wang L-D, on behalf of the Special Writing Group of China Stroke Surveillance Report, Yan F, Peng B, Hua Y, Liu M, Ji X-M, Ma L, Shan C-L, Wang Y-L, Zeng J-S, Chen H-S, Fan D-S, Gu Y-X, Tan G-J, Hu B, Kang D-Z, Liu J-M, Liu Y-L, Lou M, Luo B-Y, Pan S-Y, Wang L-H, Wu J. China stroke surveillance report 2021. Military Med Res 2023 Jul 19;10(1):33. doi: 10.1186/s40779-023-00463-x

2. Feigin VL, Stark BA, Johnson CO, Roth GA, Bisignano C, Abady GG, Abbasifard M, Abbasi-Kangevari M, Abd-Allah F, Abedi V. Global, regional, and national burden of stroke and its risk factors, 1990–2019: a systematic analysis for the Global Burden of Disease Study 2019. The Lancet Neurology Elsevier; 2021;20(10):795–820.

3. Feigin VL, Brainin M, Norrving B, Martins S, Sacco RL, Hacke W, Fisher M, Pandian J, Lindsay P. World Stroke Organization (WSO): Global Stroke Fact Sheet 2022. International Journal of Stroke 2022 Jan;17(1):18–29. doi: 10.1177/17474930211065917

4. Xu H, He K, Hu R, Ge Y, Li X, Ni F, Que B, Chen Y, Ma R. Identifying Key Biomarkers and Immune Infiltration in Female Patients with Ischemic Stroke Based on Weighted Gene Co-Expression Network Analysis. Jia X-Z, editor. Neural Plasticity 2022 Apr 8;2022:1–17. doi: 10.1155/2022/5379876

5. Morotti A, Poli L, Costa P. Acute Stroke. Semin Neurol 2019 Feb;39(01):061–072. doi: 10.1055/s-0038-1676992

6. Murray NM, Unberath M, Hager GD, Hui FK. Artificial intelligence to diagnose ischemic stroke and identify large vessel occlusions: a systematic review. Journal of neurointerventional surgery British Medical Journal Publishing Group; 2020;12(2):156–164.

7. Zhao Z, Zhang Y, Su J, Yang L, Pang L, Gao Y, Wang H. A comprehensive review for artificial intelligence on neuroimaging in rehabilitation of ischemic stroke. Frontiers in Neurology Frontiers Media SA; 2024;15:1367854.

8. Gama F, Tyskbo D, Nygren J, Barlow J, Reed J, Svedberg P. Implementation frameworks for artificial intelligence translation into health care practice: scoping review. Journal of medical Internet research JMIR Publications Toronto, Canada; 2022;24(1):e32215.

9. Van Beek EJR, Kuhl C, Anzai Y, Desmond P, Ehman RL, Gong Q, Gold G, Gulani V, Hall-Craggs M, Leiner T, Lim CCT, Pipe JG, Reeder S, Reinhold C, Smits M, Sodickson DK, Tempany C, Vargas HA, Wang M. Value of MRI in medicine: More than just another test? Magnetic Resonance Imaging 2019 Jun;49(7). doi: 10.1002/jmri.26211

10. El-Brashy MA, Mohamed HH, Ebied OM. Role of magnetic resonant diffusion-weighted imaging in evaluation of acute cerebral stroke. Menoufia Medical Journal Medknow Publications; 2014;27(4):752.

11. Wintermark M, Albers GW, Broderick JP, Demchuk AM, Fiebach JB, Fiehler J, Grotta JC, Houser G, Jovin TG, Lees KR, Lev MH, Liebeskind DS, Luby M, Muir KW, Parsons MW, Von Kummer R, Wardlaw JM, Wu O, Yoo AJ, Alexandrov AV, Alger JR, Aviv RI, Bammer R, Baron J-C, Calamante F, Campbell BCV, Carpenter TC, Christensen S, Copen WA, Derdeyn CP, Haley EC, Khatri P, Kudo K, Lansberg MG, Latour LL, Lee T-Y, Leigh R, Lin W, Lyden P, Mair G, Menon BK, Michel P, Mikulik R, Nogueira RG, Østergaard L, Pedraza S, Riedel CH, Rowley HA, Sanelli PC, Sasaki M, Saver JL, Schaefer PW, Schellinger PD, Tsivgoulis G, Wechsler LR, White PM, Zaharchuk G, Zaidat OO, Davis SM, Donnan GA, Furlan AJ, Hacke W, Kang D-W, Kidwell C, Thijs VN, Thomalla G, Warach SJ. Acute Stroke Imaging Research Roadmap II. Stroke 2013 Sep;44(9):2628–2639. doi: 10.1161/STROKEAHA.113.002015

12. Leslie-Mazwi T, Chandra RV, Fraser JF, Hoh B, Baxter BW, Albuquerque FC, Hirsch JA. AHA/ASA 2018 AIS guidelines: impact and opportunity for endovascular stroke care. Journal of neurointerventional surgery British Medical Journal Publishing Group; 2018;10(9):813–817.

13. Haggenmüller B, Kreiser K, Sollmann N, Huber M, Vogele D, Schmidt SA, Beer M, Schmitz B, Ozpeynirci Y, Rosskopf J. Pictorial review on imaging findings in cerebral CTP in patients with acute stroke and its mimics: a primer for general radiologists. Diagnostics MDPI; 2023;13(3):447.

14. Wang Y, Yao Y. Application of artificial intelligence methods in carotid artery segmentation: a review. IEEE Access IEEE; 2023; Available from: https://ieeexplore.ieee.org/

abstract/document/10038684/ [accessed Jun 13, 2024]

15. Leclerc S, Smistad E, Pedrosa J, Østvik A, Cervenansky F, Espinosa F, Espeland T, Berg EAR, Jodoin P-M, Grenier T. Deep learning for segmentation using an open large-scale dataset in 2D echocardiography. IEEE transactions on medical imaging IEEE; 2019;38(9):2198–2210.

16. Wardlaw JM, Smith EE, Biessels GJ, Cordonnier C, Fazekas F, Frayne R, Lindley RI, T O'Brien J, Barkhof F, Benavente OR. Neuroimaging standards for research into small vessel disease and its contribution to ageing and neurodegeneration. The Lancet Neurology Elsevier; 2013;12(8):822–838.

17. Parums DV. Review articles, systematic reviews, meta-analysis, and the updated preferred reporting items for systematic reviews and meta-analyses (PRISMA) 2020 guidelines. Medical science monitor: international medical journal of experimental and clinical research International Scientific Information, Inc.; 2021;27:e934475-1.

18. Cardenas CE, McCarroll RE, Court LE, Elgohari BA, Elhalawani H, Fuller CD, Kamal MJ, Meheissen MA, Mohamed AS, Rao A. Deep learning algorithm for auto-delineation of high-risk oropharyngeal clinical target volumes with built-in dice similarity coefficient parameter optimization function. International Journal of Radiation Oncology* Biology* Physics Elsevier; 2018;101(2):468–478.

19. Huttenlocher DP, Klanderman GA, Rucklidge WJ. Comparing images using the Hausdorff distance. IEEE Transactions on pattern analysis and machine intelligence IEEE; 1993;15(9):850–863.

20. Purves RD. Optimum numerical integration methods for estimation of area-under-the-curve (AUC) and area-under-the-moment-curve (AUMC). Journal of Pharmacokinetics and Biopharmaceutics 1992 Jun;20(3):211–226. doi: 10.1007/BF01062525

21. Bishop CM, Nasrabadi NM. Pattern recognition and machine learning. Springer; 2006. Available from: https://link.springer.com/in/book/9780387310732 [accessed Jun 19, 2024]

22. Shreffler J, Huecker MR. Diagnostic testing accuracy: Sensitivity, specificity, predictive values and likelihood ratios. 2020; Available from: https://europepmc.org/article/nbk/nbk557491 [accessed Jun 11, 2024]

23. Kim DY, Oh HW, Suh CH. Reporting Quality of Research Studies on AI Applications in Medical Images According to the CLAIM Guidelines in a Radiology Journal With a Strong Prominence in Asia. Korean Journal of Radiology Korean Society of Radiology; 2023;24(12):1179.

24. Lima FO, Silva GS, Furie KL, Frankel MR, Lev MH, Camargo ÉCS, Haussen DC,

Singhal AB, Koroshetz WJ, Smith WS, Nogueira RG. Field Assessment Stroke Triage for Emergency Destination: A Simple and Accurate Prehospital Scale to Detect Large Vessel Occlusion Strokes. Stroke 2016 Aug;47(8):1997–2002. doi: 10.1161/STROKEAHA.116.013301

25. Bouchez L, Sztajzel R, Vargas MI, Machi P, Kulcsar Z, Poletti P-A, Pereira VM, Lövblad K-O. CT imaging selection in acute stroke. European journal of radiology Elsevier; 2017;96:153–161.

26. Guerrero R, Qin C, Oktay O, Bowles C, Chen L, Joules R, Wolz R, Valdés-Hernández M del C, Dickie DA, Wardlaw J. White matter hyperintensity and stroke lesion segmentation and differentiation using convolutional neural networks. NeuroImage: Clinical Elsevier; 2018;17:918–934.

27. Amarenco P, Bogousslavsky J, Caplan LR, Donnan GA, Hennerici MG. Classification of stroke subtypes. Cerebrovascular diseases S. Karger AG Basel, Switzerland; 2009;27(5):493–501.

28. Gillebert CR, Humphreys GW, Mantini D. Automated delineation of stroke lesions using brain CT images. NeuroImage: Clinical Elsevier; 2014;4:540–548.

29. Matesin M, Loncaric S, Petravic D. A rule-based approach to stroke lesion analysis from CT brain images. ISPA 2001 Proceedings of the 2nd International Symposium on Image and Signal Processing and Analysis In conjunction with 23rd International Conference on Information Technology Interfaces (IEEE Cat IEEE; 2001. p. 219–223. Available from: https://ieeexplore.ieee.org/abstract/document/938631/ [accessed Jun 11, 2024]

30. Shen S, Szameitat AJ, Sterr A. An improved lesion detection approach based on similarity measurement between fuzzy intensity segmentation and spatial probability maps. Magnetic Resonance Imaging Elsevier; 2010;28(2):245–254.

31. Dayang P, Meli ASK. Evaluation of image segmentation algorithms for plant disease detection. Int J Image Graph Signal Process 2021;13:14–26.

32. Breiman L. Random forests. Machine Learning 2001;45(1):5–32. doi: 10.1023/A:1010933404324

33. Rish I. An empirical study of the naive Bayes classifier. IJCAI 2001 workshop on empirical methods in artificial intelligence Citeseer; 2001. p. 41–46. Available from: https://citeseerx.ist.psu.edu/document?repid=rep1&type=pdf&doi=2825733f97124013e8841b3f8a0f5bd4ee4af88a [accessed Jun 11, 2024]

34. Maier O, Wilms M, von der Gablentz J, Krämer U, Handels H. Ischemic stroke lesion

segmentation in multi-spectral MR images with support vector machine classifiers. Medical Imaging 2014: Computer-Aided Diagnosis SPIE; 2014. p. 21–32. Available from: https://www.spiedigitallibrary.org/conference-proceedings-of-spie/9035/903504/Ischemic-stroke-lesion-segmentation-in-multi-spectral-MR-images-with/10.1117/12.2043494.short

35. Mitra J, Bourgeat P, Fripp J, Ghose S, Rose S, Salvado O, Connelly A, Campbell B, Palmer S, Sharma G. Lesion segmentation from multimodal MRI using random forest following ischemic stroke. NeuroImage Elsevier; 2014;98:324–335.

36. Maier O, Wilms M, von der Gablentz J, Krämer UM, Münte TF, Handels H. Extra tree forests for sub-acute ischemic stroke lesion segmentation in MR sequences. Journal of neuroscience methods Elsevier; 2015;240:89–100.

37. Pustina D, Coslett HB, Turkeltaub PE, Tustison N, Schwartz MF, Avants B. Automated segmentation of chronic stroke lesions using LINDA : Lesion identification with neighborhood data analysis. Human Brain Mapping 2016 Apr;37(4):1405–1421. doi: 10.1002/hbm.23110

38. Griffis JC, Allendorfer JB, Szaflarski JP. Voxel-based Gaussian naïve Bayes classification of ischemic stroke lesions in individual T1-weighted MRI scans. Journal of neuroscience methods Elsevier; 2016;257:97–108.

39. Liu X, Song L, Liu S, Zhang Y. A review of deep-learning-based medical image segmentation methods. Sustainability MDPI; 2021;13(3):1224.

40. Goncharov M, Pisov M, Belyaev M. Ensembling Convolutional Neural Networks for Ischemic Stroke Lesion Segmentation Based on CT Images. itas2018.

41. Clèrigues A, Valverde S, Bernal J, Freixenet J, Oliver A, Lladó X. Acute ischemic stroke lesion core segmentation in CT perfusion images using fully convolutional neural networks. Computers in biology and medicine Elsevier; 2019;115:103487.

42. Wang G, Song T, Dong Q, Cui M, Huang N, Zhang S. Automatic ischemic stroke lesion segmentation from computed tomography perfusion images by image synthesis and attention-based deep neural networks. Medical Image Analysis Elsevier; 2020;65:101787.

43. Kuang H, Menon BK, Sohn SI, Qiu W. EIS-Net: segmenting early infarct and scoring ASPECTS simultaneously on non-contrast CT of patients with acute ischemic stroke. Medical Image Analysis Elsevier; 2021;70:101984.

44. Soltanpour M, Greiner R, Boulanger P, Buck B. Improvement of automatic ischemic stroke lesion segmentation in CT perfusion maps using a learned deep neural network. Computers in biology and medicine Elsevier; 2021;137:104849.

45. Luo C, Zhang J, Chen X, Tang Y, Weng X, Xu F. UCATR: Based on CNN and

transformer encoding and cross-attention decoding for lesion segmentation of acute ischemic stroke in non-contrast computed tomography images. 2021 43rd Annual International Conference of the IEEE Engineering in Medicine & Biology Society (EMBC) IEEE; 2021. p. 3565–3568. Available from: https://ieeexplore.ieee.org/abstract/document/9630336/

46. de Vries L, Emmer BJ, Majoie CB, Marquering HA, Gavves E. PerfU-net: baseline infarct estimation from CT perfusion source data for acute ischemic stroke. Medical image analysis Elsevier; 2023;85:102749.

47. Kuang H, Wang Y, Liu J, Wang J, Cao Q, Hu B, Qiu W, Wang J. Hybrid CNN-Transformer Network with Circular Feature Interaction for Acute Ischemic Stroke Lesion Segmentation on Non-contrast CT Scans. IEEE Transactions on Medical Imaging IEEE; 2024; Available from: https://ieeexplore.ieee.org/abstract/document/10423037/

48. Chen L, Bentley P, Rueckert D. Fully automatic acute ischemic lesion segmentation in DWI using convolutional neural networks. NeuroImage: Clinical Elsevier; 2017;15:633–643.

49. Zhang R, Zhao L, Lou W, Abrigo JM, Mok VC, Chu WC, Wang D, Shi L. Automatic segmentation of acute ischemic stroke from DWI using 3-D fully convolutional DenseNets. IEEE transactions on medical imaging IEEE; 2018;37(9):2149–2160.

50. Karthik R, Gupta U, Jha A, Rajalakshmi R, Menaka R. A deep supervised approach for ischemic lesion segmentation from multimodal MRI using Fully Convolutional Network. Applied Soft Computing Elsevier; 2019;84:105685.

51. Clèrigues A, Valverde S, Bernal J, Freixenet J, Oliver A, Lladó X. Acute and sub-acute stroke lesion segmentation from multimodal MRI. Computer methods and programs in biomedicine Elsevier; 2020;194:105521.

52. Wu Z, Zhang X, Li F, Wang S, Li J. TransRender: a transformer-based boundary rendering segmentation network for stroke lesions. Frontiers in Neuroscience Frontiers; 2023;17:1259677.

53. Wu Z, Zhang X, Li F, Wang S, Huang L, Li J. W-Net: A boundary-enhanced segmentation network for stroke lesions. Expert Systems with Applications Elsevier; 2023;230:120637.

54. Soh WK, Yuen HY, Rajapakse JC. HUT: Hybrid UNet transformer for brain lesion and tumour segmentation. Heliyon Elsevier; 2023;9(12). Available from: https://www.cell.com/heliyon/pdf/S2405-8440(23)09620-2.pdf

55. Inamdar MA, Raghavendra U, Gudigar A, Chakole Y, Hegde A, Menon GR, Barua P, Palmer EE, Cheong KH, Chan WY. A review on computer aided diagnosis of acute brain stroke. Sensors MDPI; 2021;21(24):8507.

56. Adam SY, Yousif A, Bashir MB. Classification of ischemic stroke using machine learning algorithms. International Journal of Computer Applications Foundation of Computer Science; 2016;149(10):26–31.

57. Gautam A, Raman B. Towards effective classification of brain hemorrhagic and ischemic stroke using CNN. Biomedical Signal Processing and Control Elsevier; 2021;63:102178.

58. Chen Y-T, Chen Y-L, Chen Y-Y, Huang Y-T, Wong H-F, Yan J-L, Wang J-J. Deep learning–based brain computed tomography image classification with hyperparameter optimization through transfer learning for stroke. Diagnostics MDPI; 2022;12(4):807.

59. Chawla M, Sharma S, Sivaswamy J, Kishore LT. A method for automatic detection and classification of stroke from brain CT images. 2009 Annual international conference of the IEEE engineering in medicine and biology society IEEE; 2009. p. 3581–3584. Available from: https://ieeexplore.ieee.org/abstract/document/5335289/

60. Barber PA, Darby DG, Desmond PM, Gerraty RP, Yang Q, Li T, Jolley D, Donnan GA, Tress BM, Davis SM. Identification of Major Ischemic Change: Diffusion-Weighted Imaging Versus Computed Tomography. Stroke 1999 Oct;30(10):2059–2065. doi: 10.1161/01.STR.30.10.2059

61. Han K, Xiao A, Wu E, Guo J, Xu C, Wang Y. Transformer in transformer. Advances in neural information processing systems 2021;34:15908–15919.

62. Wolf PA, D'Agostino RB, Belanger AJ, Kannel WB. Probability of stroke: a risk profile from the Framingham Study. Stroke 1991 Mar;22(3):312–318. doi: 10.1161/01.STR.22.3.312

63. Boehme AK, Esenwa C, Elkind MSV. Stroke Risk Factors, Genetics, and Prevention. Circulation Research 2017 Feb 3;120(3):472–495. doi: 10.1161/CIRCRESAHA.116.308398

64. Jaroslav P, Christian R, Stefan O, Alexander Z, Zepper P, Holger P, Hans-Henning E. Evaluation of Serum Biomarkers for Patients at Increased Risk of Stroke. International Journal of Vascular Medicine 2012;2012:1–6. doi: 10.1155/2012/906954

65. Saba L, Saam T, Jäger HR, Yuan C, Hatsukami TS, Saloner D, Wasserman BA, Bonati LH, Wintermark M. Imaging biomarkers of vulnerable carotid plaques for stroke risk prediction and their potential clinical implications. The Lancet Neurology Elsevier; 2019;18(6):559–572.

66. Adams HP, Bendixen BH, Kappelle LJ, Biller J, Love BB, Gordon DL, Marsh EE. Classification of subtype of acute ischemic stroke. Definitions for use in a multicenter clinical trial. TOAST. Trial of Org 10172 in Acute Stroke Treatment. Stroke 1993 Jan;24(1):35–41.

doi: 10.1161/01.STR.24.1.35

67. Flaherty ML, Kissela B, Khoury JC, Alwell K, Moomaw CJ, Woo D, Khatri P, Ferioli S, Adeoye O, Broderick JP. Carotid artery stenosis as a cause of stroke. Neuroepidemiology S. Karger AG Basel, Switzerland; 2012;40(1):36–41.

68. Raghib MF, Mutzenbach JS, Rösler C, Otto F, Mc Coy M, Müller-Thies-Broussalis E, Pikija S. Acute treatment of stroke due to spontaneous calcified cerebral emboli causing large vessel occlusion. Journal of Clinical Neuroscience Elsevier; 2018;47:56–61.

69. Casaclang-Verzosa G, Gersh BJ, Tsang TSM. Structural and Functional Remodeling of the Left Atrium. Journal of the American College of Cardiology 2008 Jan;51(1):1–11. doi: 10.1016/j.jacc.2007.09.026

70. Caprio FZ, Lin C. Unusual causes of ischemic stroke and transient ischemic attack. Warlow's Stroke: Practical Management John Wiley & Sons; 2019;4202676.

71. Alexandratou M, Papachristodoulou A, Li X, Partovi S, Davidhi A, Rafailidis V, Prassopoulos P, Kamperidis V, Koutroulou I, Tsivgoulis G. Advances in noninvasive carotid wall imaging with ultrasound: a narrative review. Journal of Clinical Medicine MDPI; 2022;11(20):6196.

72. Jaff MR, Goldmakher GV, Lev MH, Romero JM. Imaging of the carotid arteries: the role of duplex ultrasonography, magnetic resonance arteriography, and computerized tomographic arteriography. Vasc Med 2008 Nov;13(4):281–292. doi: 10.1177/1358863X08091971

73. Alam J, Hassan M, Khan A, Chaudhry A. Robust fuzzy RBF network based image segmentation and intelligent decision making system for carotid artery ultrasound images. Neurocomputing Elsevier; 2015;151:745–755.

74. Araki T, Jain PK, Suri HS, Londhe ND, Ikeda N, El-Baz A, Shrivastava VK, Saba L, Nicolaides A, Shafique S. Stroke risk stratification and its validation using ultrasonic echolucent carotid wall plaque morphology: a machine learning paradigm. Computers in biology and medicine Elsevier; 2017;80:77–96.

75. Al-Mohannadi A, Al-Maadeed S, Elharrouss O, Sadasivuni KK. Encoder-decoder architecture for ultrasound IMC segmentation and cIMT measurement. Sensors MDPI; 2021;21(20):6839.

76. Mi S, Bao Q, Wei Z, Xu F, Yang W. MBFF-Net: Multi-Branch Feature Fusion Network for Carotid Plaque Segmentation in Ultrasound. In: De Bruijne M, Cattin PC, Cotin S, Padoy N, Speidel S, Zheng Y, Essert C, editors. Medical Image Computing and Computer Assisted Intervention – MICCAI 2021 Cham: Springer International Publishing; 2021. p.

313–322. doi: 10.1007/978-3-030-87240-3_30

77. Latha S, Muthu P, Lai KW, Khalil A, Dhanalakshmi S. Performance analysis of machine learning and deep learning architectures on early stroke detection using carotid artery ultrasound images. Frontiers in Aging Neuroscience Frontiers; 2022;13:828214.

78. Jiang M, Chiu B. A dual-stream centerline-guided network for segmentation of the common and internal carotid arteries from 3D ultrasound images. IEEE Transactions on Medical Imaging IEEE; 2023; Available from: https://ieeexplore.ieee.org/abstract/document/10089861/

79. Degel MA, Navab N, Albarqouni S. Domain and Geometry Agnostic CNNs for Left Atrium Segmentation in 3D Ultrasound. In: Frangi AF, Schnabel JA, Davatzikos C, Alberola-López C, Fichtinger G, editors. Medical Image Computing and Computer Assisted Intervention – MICCAI 2018 Cham: Springer International Publishing; 2018. p. 630–637. doi: 10.1007/978-3-030-00937-3_72

80. Moradi S, Oghli MG, Alizadehasl A, Shiri I, Oveisi N, Oveisi M, Maleki M, Dhooge J. MFP-Unet: A novel deep learning based approach for left ventricle segmentation in echocardiography. Physica Medica Elsevier; 2019;67:58–69.

81. Leclerc S, Smistad E, Grenier T, Lartizien C, Ostvik A, Cervenansky F, Espinosa F, Espeland T, Berg EAR, Jodoin P-M. RU-Net: A refining segmentation network for 2D echocardiography. 2019 IEEE International Ultrasonics Symposium (IUS) IEEE; 2019. p. 1160–1163. Available from: https://ieeexplore.ieee.org/abstract/document/8926158/

82. Liu F, Wang K, Liu D, Yang X, Tian J. Deep pyramid local attention neural network for cardiac structure segmentation in two-dimensional echocardiography. Medical Image Analysis Elsevier; 2021;67:101873.

83. Li H, Wang Y, Qu M, Cao P, Feng C, Yang J. EchoEFNet: multi-task deep learning network for automatic calculation of left ventricular ejection fraction in 2D echocardiography. Computers in Biology and Medicine Elsevier; 2023;156:106705.

84. Debette S, Markus HS. The clinical importance of white matter hyperintensities on brain magnetic resonance imaging: systematic review and meta-analysis. Bmj British Medical Journal Publishing Group; 2010;341. Available from: https://www.bmj.com/content/341/bmj.c3666.abstract [accessed Jun 17, 2024]

85. Das AS, Regenhardt RW, Vernooij MW, Blacker D, Charidimou A, Viswanathan A. Asymptomatic cerebral small vessel disease: insights from population-based studies. Journal of stroke Korean Stroke Society; 2019;21(2):121.

86. Liu L, Chen S, Zhu X, Zhao X-M, Wu F-X, Wang J. Deep convolutional neural

network for accurate segmentation and quantification of white matter hyperintensities. Neurocomputing Elsevier; 2020;384:231–242.

87. Park G, Hong J, Duffy BA, Lee J-M, Kim H. White matter hyperintensities segmentation using the ensemble U-Net with multi-scale highlighting foregrounds. Neuroimage Elsevier; 2021;237:118140.

88. Li X, Zhao Y, Jiang J, Cheng J, Zhu W, Wu Z, Jing J, Zhang Z, Wen W, Sachdev PS, Wang Y, Liu T, Li Z. White matter hyperintensities segmentation using an ensemble of neural networks. Human Brain Mapping 2022 Feb 15;43(3):929–939. doi: 10.1002/hbm.25695

89. Huang F, Xia P, Vardhanabhuti V, Hui S, Lau K, Ka-Fung Mak H, Cao P. Semisupervised white matter hyperintensities segmentation on MRI. Human Brain Mapping 2023 Mar;44(4):1344–1358. doi: 10.1002/hbm.26109

90. Farkhani S, Demnitz N, Boraxbekk C-J, Lundell H, Siebner HR, Petersen ET, Madsen KH. End-to-end volumetric segmentation of white matter hyperintensities using deep learning. Computer Methods and Programs in Biomedicine Elsevier; 2024;245:108008.

91. Ertl M, Meisinger C, Linseisen J, Baumeister S-E, Zickler P, Naumann M. Long-term outcomes in patients with stroke after in-hospital treatment—Study protocol of the prospective stroke cohort Augsburg (SCHANA study). Medicina MDPI; 2020;56(6):280.

92. Desmurget M, Bonnetblanc F, Duffau H. Contrasting acute and slow-growing lesions: a new door to brain plasticity. Brain Oxford University Press; 2007;130(4):898–914.

93. McKinley R, Häni L, Gralla J, El-Koussy M, Bauer S, Arnold M, Fischer U, Jung S, Mattmann K, Reyes M, Wiest R. Fully automated stroke tissue estimation using random forest classifiers (FASTER). J Cereb Blood Flow Metab 2017 Aug;37(8):2728–2741. doi: 10.1177/0271678X16674221

94. Nielsen A, Hansen MB, Tietze A, Mouridsen K. Prediction of Tissue Outcome and Assessment of Treatment Effect in Acute Ischemic Stroke Using Deep Learning. Stroke 2018 Jun;49(6):1394–1401. doi: 10.1161/STROKEAHA.117.019740

95. Yu Y, Xie Y, Thamm T, Gong E, Ouyang J, Huang C, Christensen S, Marks MP, Lansberg MG, Albers GW. Use of deep learning to predict final ischemic stroke lesions from initial magnetic resonance imaging. JAMA network open American Medical Association; 2020;3(3):e200772–e200772.

96. Pinto A, Pereira S, Meier R, Wiest R, Alves V, Reyes M, Silva CA. Combining unsupervised and supervised learning for predicting the final stroke lesion. Medical image analysis Elsevier; 2021;69:101888.

97. Wong KK, Cummock JS, Li G, Ghosh R, Xu P, Volpi JJ, Wong STC. Automatic

Segmentation in Acute Ischemic Stroke: Prognostic Significance of Topological Stroke Volumes on Stroke Outcome. Stroke 2022 Sep;53(9):2896–2905. doi: 10.1161/STROKEAHA.121.037982

98. Beloosesky Y, Streifler JY, Burstin A, Grinblat J. The importance of brain infarct size and location in predicting outcome after stroke. Age and ageing Oxford University Press; 1995;24(6):515–518.

99. Bentley P, Ganesalingam J, Jones ALC, Mahady K, Epton S, Rinne P, Sharma P, Halse O, Mehta A, Rueckert D. Prediction of stroke thrombolysis outcome using CT brain machine learning. NeuroImage: Clinical Elsevier; 2014;4:635–640.

100. Monteiro M, Fonseca AC, Freitas AT, e Melo TP, Francisco AP, Ferro JM, Oliveira AL. Using machine learning to improve the prediction of functional outcome in ischemic stroke patients. IEEE/ACM transactions on computational biology and bioinformatics IEEE; 2018;15(6):1953–1959.

101. Cheon S, Kim J, Lim J. The use of deep learning to predict stroke patient mortality. International journal of environmental research and public health MDPI; 2019;16(11):1876.

102. Kuang H, Najm M, Chakraborty D, Maraj N, Sohn SI, Goyal M, Hill MD, Demchuk AM, Menon BK, Qiu W. Automated ASPECTS on noncontrast CT scans in patients with acute ischemic stroke using machine learning. American journal of neuroradiology Am Soc Neuroradiology; 2019;40(1):33–38.

103. Scrutinio D, Ricciardi C, Donisi L, Losavio E, Battista P, Guida P, Cesarelli M, Pagano G, D'Addio G. Machine learning to predict mortality after rehabilitation among patients with severe stroke. Scientific reports Nature Publishing Group UK London; 2020;10(1):20127.

104. Brugnara G, Neuberger U, Mahmutoglu MA, Foltyn M, Herweh C, Nagel S, Schönenberger S, Heiland S, Ulfert C, Ringleb PA, Bendszus M, Möhlenbruch MA, Pfaff JAR, Vollmuth P. Multimodal Predictive Modeling of Endovascular Treatment Outcome for Acute Ischemic Stroke Using Machine-Learning. Stroke 2020 Dec;51(12):3541–3551. doi: 10.1161/STROKEAHA.120.030287

105. Fang G, Huang Z, Wang Z. Predicting ischemic stroke outcome using deep learning approaches. Frontiers in genetics Frontiers Media SA; 2022;12:827522.

106. Bivard A, Churilov L, Parsons M. Artificial intelligence for decision support in acute stroke—current roles and potential. Nature Reviews Neurology Nature Publishing Group UK London; 2020;16(10):575–585.

107. Recht MP, Dewey M, Dreyer K, Langlotz C, Niessen W, Prainsack B, Smith JJ.

Integrating artificial intelligence into the clinical practice of radiology: challenges and recommendations. Eur Radiol 2020 Jun;30(6):3576–3584. doi: 10.1007/s00330-020-06672-5

108. Mazurowski MA, Dong H, Gu H, Yang J, Konz N, Zhang Y. Segment anything model for medical image analysis: an experimental study. Medical Image Analysis Elsevier; 2023;89:102918.

109. Zhu L, Liao B, Zhang Q, Wang X, Liu W, Wang X. Vision Mamba: Efficient Visual Representation Learning with Bidirectional State Space Model. arXiv; 2024. Available from: http://arxiv.org/abs/2401.09417

110. Meskó B. The impact of multimodal large language models on health care's future. Journal of Medical Internet Research JMIR Publications Toronto, Canada; 2023;25:e52865.

111. Ma J, He Y, Li F, Han L, You C, Wang B. Segment anything in medical images. Nature Communications Nature Publishing Group UK London; 2024;15(1):654.

112. Li Y, Jing B, Li Z, Wang J, Zhang Y. nnSAM: Plug-and-play Segment Anything Model Improves nnUNet Performance. arXiv; 2024. Available from: http://arxiv.org/abs/2309.16967

113. Elyoseph Z, Levkovich I, Shinan-Altman S. Assessing prognosis in depression: comparing perspectives of AI models, mental health professionals and the general public. Family Medicine and Community Health BMJ Publishing Group; 2024;12(Suppl 1). Available from: https://www.ncbi.nlm.nih.gov/pmc/articles/PMC10806564/

114. Chen Z, Balan MM, Brown K. Language Models are Few-shot Learners for Prognostic Prediction. arXiv; 2023. Available from: http://arxiv.org/abs/2302.12692

115. Gu Z, He X, Yu P, Jia W, Yang X, Peng G, Hu P, Chen S, Chen H, Lin Y. Automatic quantitative stroke severity assessment based on Chinese clinical named entity recognition with domain-adaptive pre-trained large language model. Artificial Intelligence in Medicine Elsevier; 2024;102822.

116. Li L, Fan Y, Tse M, Lin K-Y. A review of applications in federated learning. Computers & Industrial Engineering Elsevier; 2020;149:106854.

117. Deniz-Garcia A, Fabelo H, Rodriguez-Almeida AJ, Zamora-Zamorano G, Castro-Fernandez M, Alberiche Ruano M del P, Solvoll T, Granja C, Schopf TR, Callico GM. Quality, usability, and effectiveness of mHealth apps and the role of artificial intelligence: current scenario and challenges. Journal of Medical Internet Research JMIR Publications Toronto, Canada; 2023;25:e44030.

Supplementary Files

Figures

AI for diagnosing acute stroke over the past 25 years.

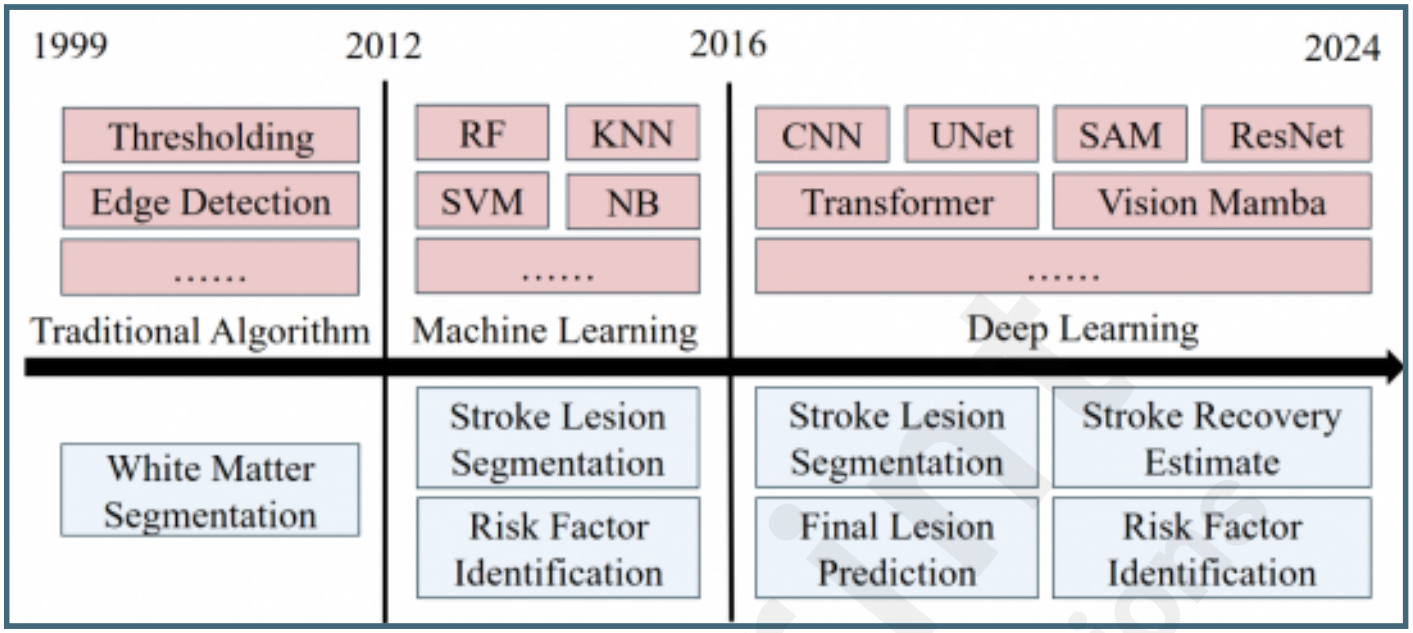

Stroke lesions identified using different imaging modalities. (A)NCCT; (B)CTP; (C)T1WI; (D)T2WI; (E)FLAIR; (F)DWI (G)NCCT (annotated); (H)CTP (annotated); (I)T1WI (annotated); (J)T2WI (annotated); (K)FLAIR (annotated); (L)DWI (annotated). Stroke lesion areas are marked with blue regions and the images are not paired.

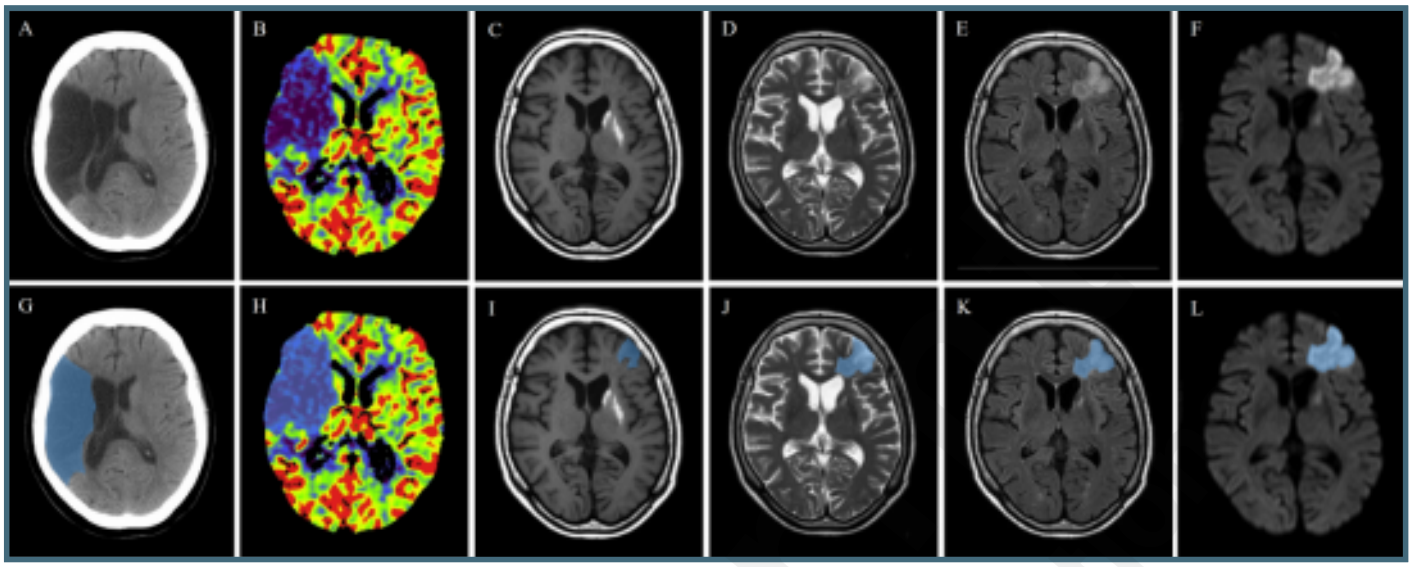

Cardiac US and carotid US. (A) Cardiac US (two heart chambers); (B) Cardiac US (four heart chambers); (C) 3D Carotid US; (D) 2D Carotid US.

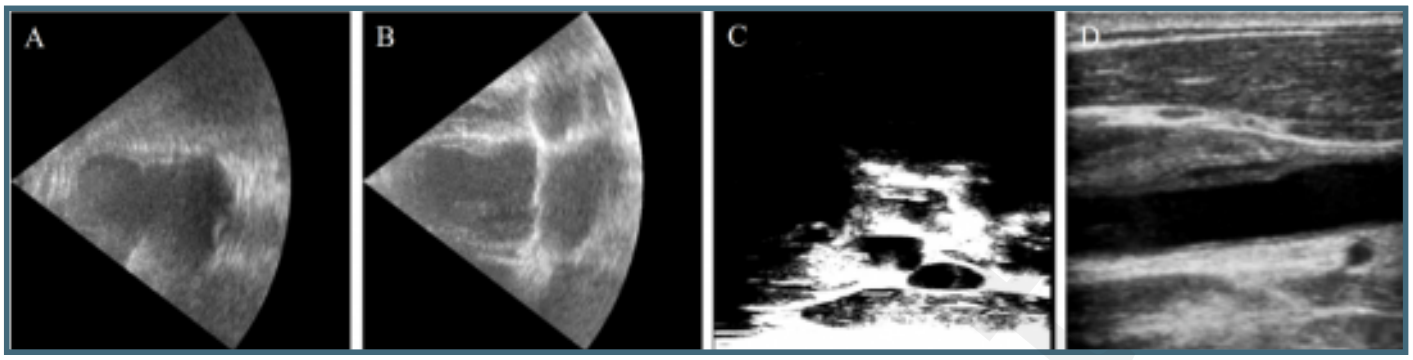

PRISMA flowchart for systematic filtering and selection of articles.

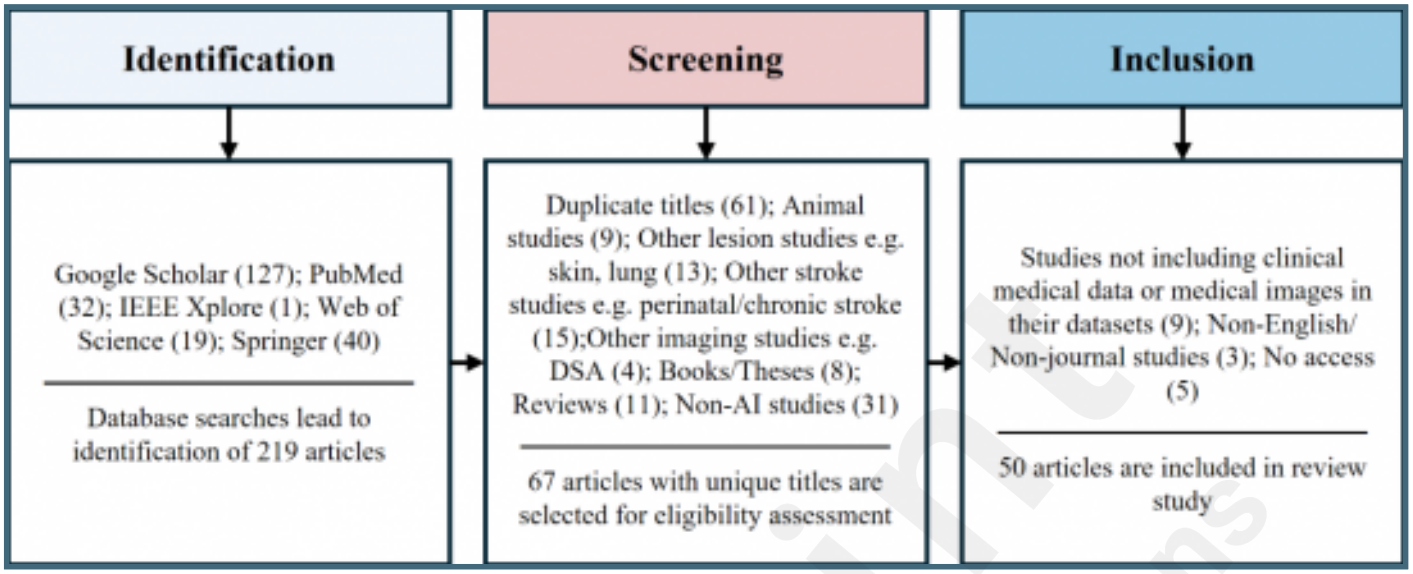

Ischemic stroke and hemorrhagic stroke. (A) Ischemic stroke; (B) Ischemic stroke (annotated); (C) Hemorrhagic stroke; (D) Hemorrhagic stroke (annotated). Stroke lesion areas are marked with blue regions.

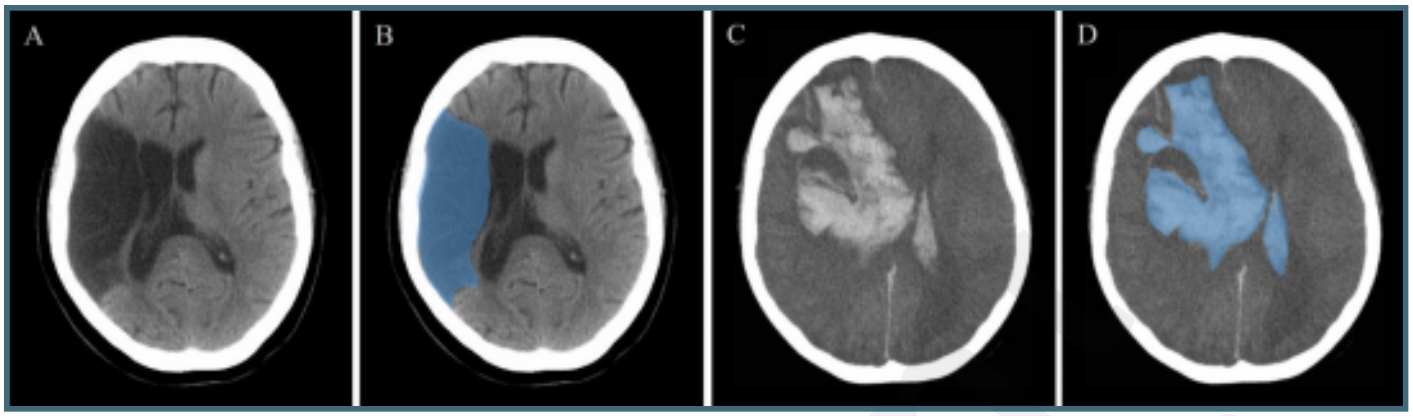

Risk factors and etiology of stroke. (A) Hemorrhagic stroke and Ischemic stroke; (B) LAA-type stroke and its risk factors; (C) CE-type stroke and its risk factors; (D) SAO-type stroke and its risk factors.

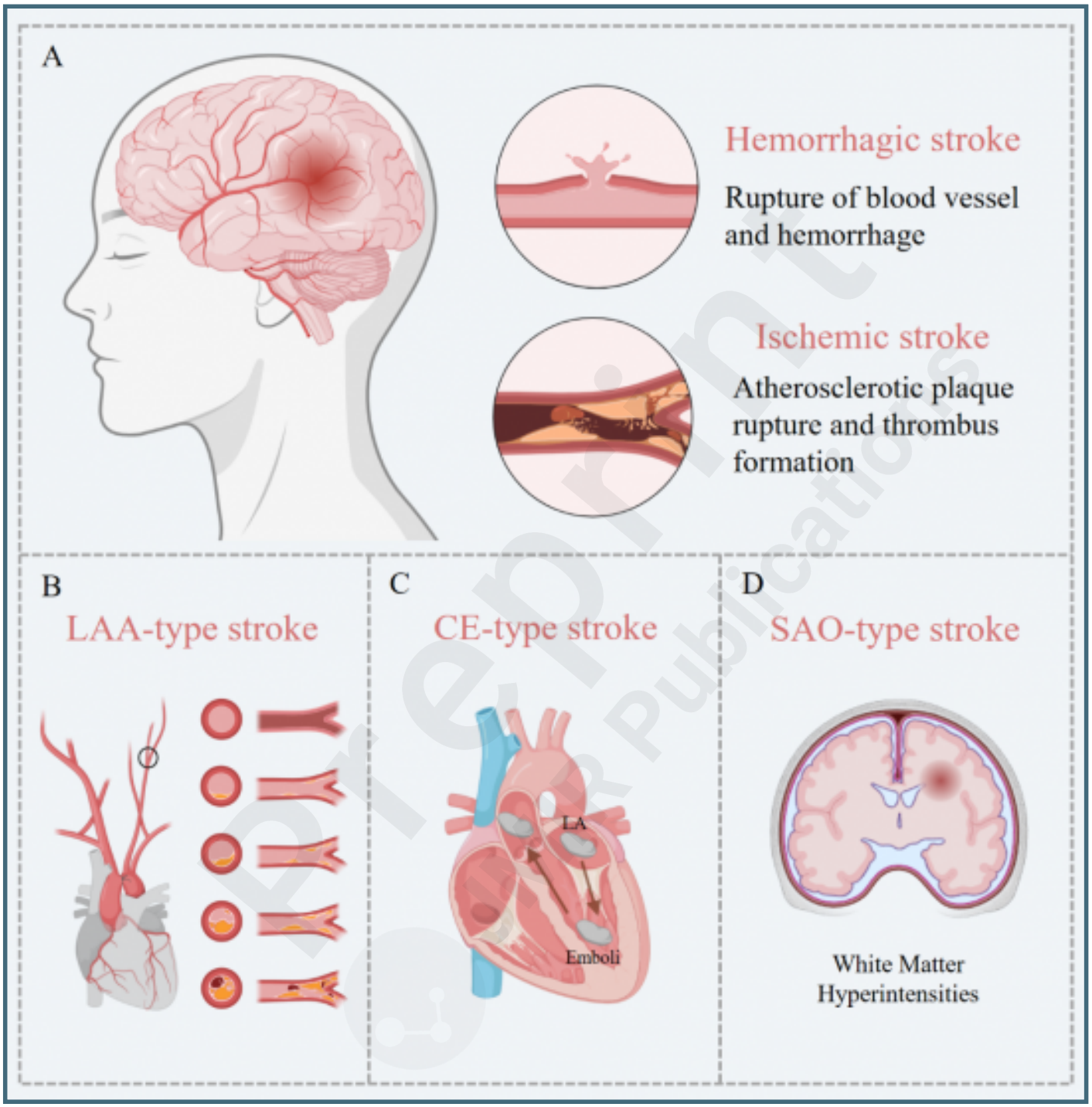

Carotid artery stenosis. (A) Health people; (B) Health people (annotated); (C) Patient with CAS; (D) Patient with CAS (annotated). Lumens are marked with blue regions.

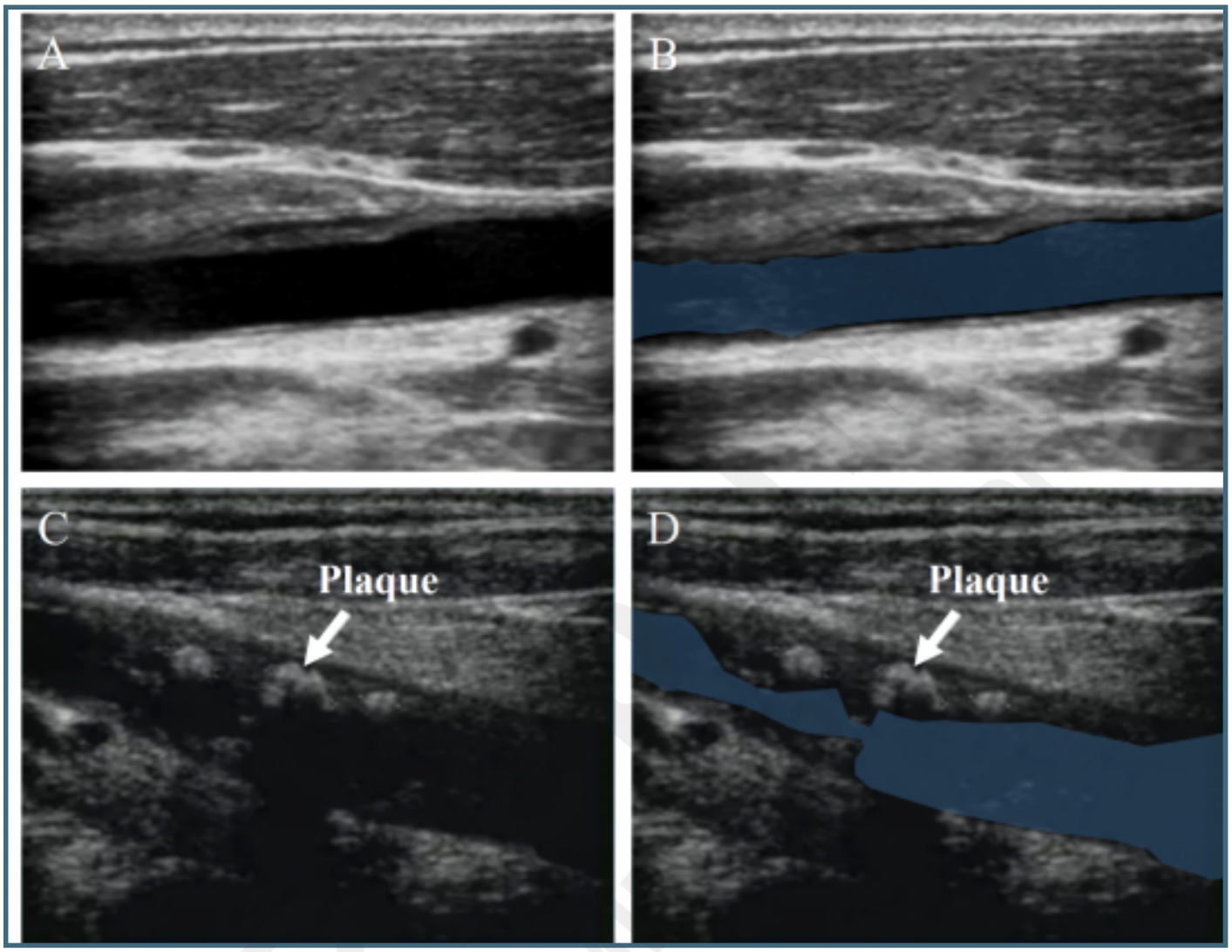

The presence of LA enlargement. (A) Health people; (B) Health people (annotated); (C) Patient with LA enlargement; (D) Patient with LA enlargement (annotated). LA areas are marked with blue regions.

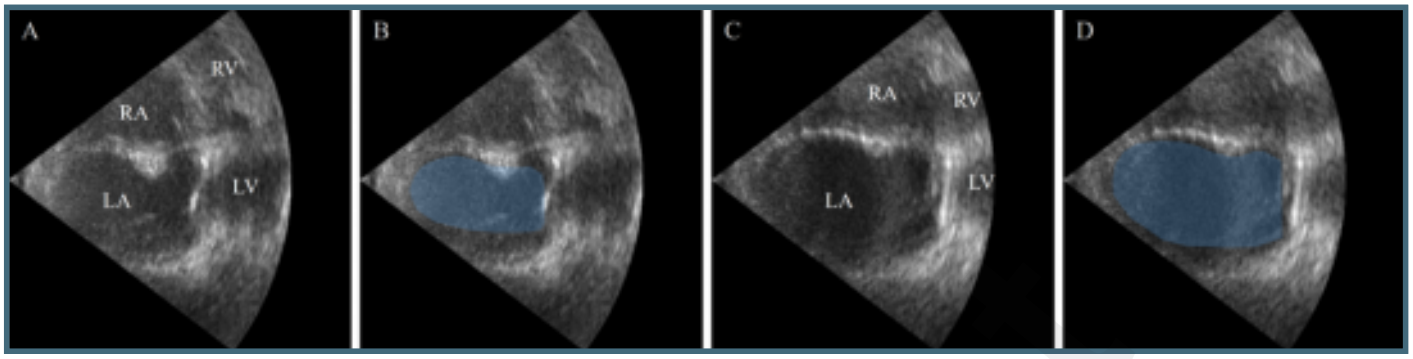

The presence of WMH. (A) Patient with minor WMH; (B) Patient with minor WMH (an-notated); (C) Patient with extensive WMH; (D) Patient with extensive WMH (annotated). WMH areas are marked with blue regions.